

1 Do Fe-Ti-oxide magmas exist? Probably not! *Revision 1 (June 7, 2017)*

2  
3 Donald H. Lindsley<sup>1</sup> and Nathan Epler<sup>2</sup>

4  
5 <sup>1</sup>Department of Geosciences, Stony Brook University, Stony Brook, NY 11794-2100.

6 [donald.lindsley@stonybrook.edu](mailto:donald.lindsley@stonybrook.edu). <sup>2</sup>Roux Associates, 209 Shafter Street, Islandia, NY 11749  
7 nepler@rouxinc.com

8  
9 **ABSTRACT**

10  
11 Many Fe-Ti oxide bodies associated with anorthosite suites and with some tholeiitic  
12 plutonic bodies have cross-cutting relationships with their host rocks suggesting that they may  
13 have been emplaced as oxide melts. Pure Fe-Ti oxides melt at temperatures much higher than  
14 is considered to be geologically realistic, so various fluxes (mainly apatite, fluorine, or carbon)  
15 have been called upon to stabilize the melts down to plausible temperatures. This review traces  
16 our experimental attempts to test the effectiveness of proposed fluxes and therefore to  
17 demonstrate the existence of such melts at geologically realistic temperatures.

18  
19 Neither F-apatite nor carbon act to stabilize Ti-rich Fe-Ti oxide melts at 1300°C and  
20 below, and we conclude that - unless some totally unforeseen material does serve as a flux -  
21 Fe-Ti oxide magmas almost certainly do not exist. Although our data are not conclusive, it  
22 appears that increasing contents of FeO (and possibly TiO<sub>2</sub>) and P<sub>2</sub>O<sub>5</sub> mutually enhance their  
23 solubilities in silicate melts, allowing extensive build-up of those components in melts residual  
24 to anorthosite. We interpret that oxide orebodies form by gravitational accumulation of  
25 crystalline oxides from such liquids. Once those melts become saturated with either Fe-Ti oxides  
26 or apatite, both phases will tend to co-precipitate, thus explaining the common occurrence of  
27 apatite with oxide orebodies (“nelsonites”. Cross-cutting oxide bodies were probably  
28 emplaced as crystalline oxides, possibly lubricated by small amounts of residual silicate liquid.  
29 Oxidation of the Fe<sub>2</sub>TiO<sub>4</sub> component in initially ulvospinel-rich spinel and concomitant  
30 formation of ilmenite grains by granule-oxy-“exsolution” may have weakened the crystalline

31 oxide and facilitated its flow during emplacement.

32 It seems clear, though, that the presence of carbon does stabilize *Ti-poor* iron oxide melts  
33 to very low temperatures (at and even below 1000°C), consistent with the (disputed!) magmatic  
34 origin of the magnetite lavas at El Laco, Chile.

35

36 Keywords: Fe-Ti oxides, oxide melts, oxide magmas, orebodies, immiscible melts, anorthosite  
37 suite, apatite, flux.

38

### 39 INTRODUCTION

40

41 Large bodies of Fe-Ti oxides (mainly titaniferous magnetite and ilmenite) are important  
42 sources of titanium and are also significant reserves of iron (see, for example, Gross, 1996; and  
43 especially the comprehensive reviews by Woodruff et al., 2013, and by Charlier et al., 2015).  
44 Their almost universal association with Proterozoic massif anorthosites strongly suggests a  
45 genetic relation to the anorthositic suite - anorthosites plus spatially- and temporally-associated  
46 rocks that go by a wide variety of names, including ferrodiorites (jotunites), syenites and  
47 monzodiorites (broadly mangerites), and high-K granites (charnockites). Many of these oxide  
48 bodies contain apatite in varying amounts, and the more apatite-rich ones are sometimes called  
49 “nelsonites” despite the fact that the type nelsonite is an ilmenite-apatite rock with essentially no  
50 magnetite (Watson, 1907, p. 300). It is probably fair to say that most workers today accept that  
51 the oxide bodies formed from melts residual to the anorthosites, but there is broad disagreement  
52 as to just how they formed and whether the oxides separated and were concentrated as **crystals**  
53 or as **immiscible oxide melts**. Some form “conformable layers...within oxide-rich gabbros”,  
54 but many are “massive ore bodies that exhibit sharp, irregular contacts with surrounding ...  
55 anorthosites” (Ashwal, 1993, p. 157). It is the latter, cross-cutting type of occurrence that has  
56 led many workers to conclude that the oxides were emplaced as liquids, presumably liquids  
57 immiscible with a corresponding silicate melt. Asklund (1949) proposed that the *Ti-poor* oxides  
58 at Kiruna formed from an immiscible iron oxide-apatite melt. Buddington et al. (1955)  
59 considered the possibility that Fe-Ti oxide deposits may have formed as immiscible oxide  
60 liquids, but considered the evidence inconclusive. Perhaps the first worker to propose the

61 existence of **immiscible** Fe-Ti oxide liquids was Hargraves (1962, p. 175) who stated “Despite  
62 the lack of any sound experimental or theoretical foundation, immiscibility between silicate-rich  
63 and oxide-rich phases [context suggests this refers to melts] is suggested.” Noting that the  
64 Allard Lake oxide ores typically contain 8-10 wt % apatite, Hargraves further suggested that  
65 significant amounts of apatite component had dissolved in the proposed oxide melt, thereby  
66 stabilizing it. Bateman (1951) had earlier suggested the existence of Fe-Ti- rich melts, but he  
67 viewed these as simply the residual melts after extensive silicate crystallization (evidently his  
68 interpretation of “petrogeny’s residua system”), not melts immiscible with coexisting silicate  
69 liquids. It may be important here to emphasize that - like the data reviewed and presented here -  
70 this paper is mute on the possible importance of *silicate*-liquid immiscibility as a petrologic  
71 process. It is restricted to experimental evidence for and against the existence of Fe-Ti oxide  
72 melts - which by implication would have coexisted with one or more silicate liquids.

73  
74 An apparent experimental foundation for the existence of immiscible oxide liquids was  
75 provided by Philpotts (1967) who heated a mixture of apatite, magnetite, and diorite in air to  
76 1420 °C and produced *three* immiscible liquids, one of which contained approximately two parts  
77 Fe<sub>3</sub>O<sub>4</sub> component to one part apatite component (with a small silicate content as well). That  
78 composition is sometimes called the “nelsonite eutectic”, and Philpotts’ work continues to be  
79 cited by those favoring the immiscible-oxide-melt hypothesis despite the fact that this melt  
80 contains no TiO<sub>2</sub> (except a minute contribution from the diorite) and the temperature (1420 °C)  
81 is approximately 200-250 °C higher than modern geothermometry would suggest for the oxide  
82 bodies and associated silicate rocks. Possible evidence supporting this “eutectic” was provided  
83 by Kolker (1982) who showed that - while there is a wide range - in a number of nelsonites the  
84 ratio of modal oxides to apatite is broadly centered around 2:1.

85  
86 The strongest evidence in favor of immiscible Fe-Ti oxide melts continues to be the  
87 clearly cross-cutting, dike-like, relationships between many oxide bodies and the host rocks  
88 (usually anorthosite). For example, in the authors’ own experience, almost every geologist who  
89 has seen those relationships in the Laramie (Wyoming) anorthosite complex (Sybille Pit; Iron  
90 Mountain; Shanton deposit) has accepted that the oxides were emplaced as liquids. The only

91 voiced exception was Lew Ashwal, who argued for emplacement as a crystalline mush (see also  
92 Ashwal, 1978). Variations of that latter hypothesis have also been advocated by Emslie (1975),  
93 Duchesne (1996; 1999); Dymek and Owens (2002), and Charlier et al (2015).

94 Detailed mapping in the Laramie anorthosite complex by Eberle (1983) of the Iron  
95 Mountain deposit (which occurs within in the Chugwater anorthosite (Lindsley et al., 2010)) and  
96 by Bolsover (1986) of the Sybille Pit (which occurs within the Poe Mountain anorthosite  
97 (Scoates et al., 2010)) led both of them to conclude that the oxides had been emplaced by  
98 downward-intruding Fe-Ti oxide melts. They both also noted the presence of oxide-rich  
99 troctolitic rocks in these deposits, and suggested that those rocks might represent the  
100 complementary silicate melts from which the proposed immiscible oxide melts separated. Both  
101 the oxides and the troctolites contain distinct, but highly variable, amounts of apatite (Bolsover  
102 reported 0 to 56 volume % apatite in her samples). Bolsover described an exposure showing  
103 oxide-poor troctolite at the top, grading downwards to nearly pure Fe-Ti oxide ore at the base.  
104 A xenolith of anorthosite within the troctolite has a layer of nearly pure oxide on its upper  
105 surface. The outcrop presented clear evidence of gravity segregation of the denser oxides -  
106 regardless of whether they separated as crystals or as immiscible oxide melt. (This beautiful  
107 outcrop has sadly been mainly obliterated by “reclamation” of the Sybille Pit in the 1990s).

108  
109 **Oxide mineralogy.** The dominant oxide mineral at both Iron Mountain and Sybille is  
110 titaniferous magnetite. In a few cases the magnetite host lacks ilmenite lamellae but contains  
111 separate (100) lamellae of ulvospinel and of green hercynitic spinel. However, in most samples  
112 the magnetite contains lamellae of ilmenite in (111), together with interstitial grains of ilmenite;  
113 hercynitic spinel occurs both as individual grains and as (100) lamellae in the magnetite. The  
114 ilmenite lamellae were interpreted as having formed by oxy-“exsolution” of ulvospinel  
115 component during cooling; there is a possibility that some or even all the separate ilmenite grains  
116 had also once been part of the spinel (forming by granule oxy-“exsolution”; Buddington and  
117 Lindsley, 1964). Bolsover noted a negative correlation between the relative modal abundance  
118 of ilmenite grains and the  $\text{TiO}_2$  content of the magnetite, and suggested that the original oxide  
119 phase may have been a  $\text{Fe}_2\text{TiO}_4$ -rich spinel (having 5-10%  $(\text{Fe,Mg})\text{Al}_2\text{O}_4$  component), with little  
120 or no primary ilmenite present.



151 to use natural samples from the Sybille Pit. One was Bolsover's sample SCP-113 (hereafter  
152 ORT), an oxide-rich troctolite containing titaniferous magnetite with (111) lamellae of ilmenite  
153 and blebs of hercynitic spinel, separate ilmenite grains, olivine, and plagioclase, with minor  
154 apatite. This sample was suggested by Bolsover (1986) as possibly representative of the  
155 composition from which both silicate and Fe-Ti oxide melts had unmixed. The other (here  
156 called ORE) was a sample of oxide ore containing ~85 % titaniferous magnetite with (100)  
157 lamellae of both ulvospinel and hercynitic spinel and ~15% plagioclase and olivine). Both  
158 samples were crushed and then ground in an agate mortar to produce powders with maximum  
159 grain sizes of 20-30 microns. A portion of the ORT powder was then reduced at 1040°C in a  
160 CO-CO<sub>2</sub> mixture to produce an  $fO_2$  value "within the fayalite stability field" (Epler, 1987).  
161 Both reduced and unreduced ORT powders were used in the experiments. Because phosphate  
162 and carbon had been proposed as possible fluxes for oxide melts, Epler added a natural  
163 fluorapatite (Durango; Young et al., 1969), synthetic iron phosphate (Fe<sub>3</sub>(P<sub>2</sub>O<sub>7</sub>)<sub>3</sub>), oxalic acid  
164 dihydrate, and/or graphite to many of his experiments.

165  
166 **Experimental details.** Epler faced several experimental challenges. Available  
167 geobarometry suggested emplacement pressures near 0.3 GPa for the Sybille deposit (e.g.,  
168 Fuhrman et al. 1988), but at the time we believed that piston-cylinder experiments could not  
169 reliably be conducted below 0.5 GPa, so he chose that pressure for his experiments.  
170 Furthermore, we were still using ½" (12.5 mm) Boyd-England (1963) talc/boron nitride cells at  
171 that time, and their geometry limited the *outer* diameter of the sample capsule to 2.4 mm.  
172 Choice of sample capsule was limited because of the high Fe content of the samples. Silver is  
173 essentially immiscible with iron, but its melting temperature is too low to be useful. Iron  
174 capsules would have imposed an unrealistically low  $fO_2$ . The size constraint precluded use of  
175 platinum-jacketed graphite capsules. Epler used platinum capsules, and since pure Pt readily  
176 alloys with Fe, he painstakingly "pre-soaked" each capsule with iron (the amount determined by  
177 trial and error) so as to minimize Fe loss or gain during the melting experiments (see Chen and  
178 Lindsley, 1983). The experiments were carried out at 1060, 1100, 1150, and 1200°C, a range  
179 thought to include the likely temperatures of emplacement, and were quenched by turning off the  
180 power to the assembly. As in all piston-cylinder experiments, "quench" is a relative term; Epler

181 estimated that the samples reached subsolidus temperatures in less than 3 seconds.

182

183 **Epler's results.**

184

185 The one experiment on ORT at 1060°C appeared to be subsolidus, with no evidence for  
186 melting of either the silicate or oxide portion. However, the titaniferous magnetite and ilmenite  
187 in the starting material did homogenize to a single spinel in that experiment, thereby providing  
188 support for Bolsover's suggestion that there may have been only one primary oxide phase in the  
189 Sybille rocks. Although the Fe-Ti oxides homogenized, they did not increase significantly in  
190 grain size, in contrast to experiments conducted at higher temperatures.

191

192 All experiments at 1100°C and above underwent partial melting, producing silicate melt  
193 that quenched to glass in 1100°C experiments, but formed glass interlaced with feathery Fe-Ti  
194 oxide minerals in those performed at higher temperatures. All also produced primary Fe-Ti  
195 oxides showing a wide variety of textures, some of which were highly suggestive of having been  
196 immiscible droplets. Importantly, there was a significant increase in oxide grain size (2-3x or  
197 more) relative to the starting material. The experiments at 1100°C also yielded primary olivine,  
198 which was absent from experiments at higher temperatures. Proportions of phases (Fig. 1) were  
199 determined by point-counting.

200

201 **Textures.** Oxide melts are essentially impossible to quench successfully to glass; they  
202 inevitably crystallize upon cooling. Therefore one must use indirect evidence - such as textures  
203 - to deduce the former existence of oxide melt at the temperature of an experiment. Some  
204 typical textures of Epler's experiments are shown in Figs. 2 A-F. Many oxides are at least  
205 partly rounded, and some even wrap around vesicles (Fig. 2D). Epler - with the agreement of  
206 his advisor - interpreted the oxide textures as indicating the presence of immiscible oxide melt  
207 droplets at the temperatures of the experiments. We interpreted the partial euhedral outlines of  
208 many grains as the result of quench overgrowth from the surrounding silicate melt during  
209 cooling of the experiment; in some experiments (e.g., Fig 2C, F), the scarcity of feathery oxides  
210 in the silicate glass immediately adjacent to primary oxide grains supported that hypothesis. We

211 interpreted the increase in grain size (over that of the starting material) as having resulted from  
212 the coalescence of melted oxide droplets, although we could not rule out simple grain ripening of  
213 unmelted oxides during the course of the experiment.

214  
215 **Oxide chemistry.** Epler was very careful to point out that only the **textures** provided  
216 evidence for the formation of immiscible oxide melts in his experiments. If immiscible oxide  
217 and silicate melts did coexist, the chemical potentials of all components should have been the  
218 same in both melts at the temperatures of the experiment, although the amounts of “lithophile”  
219 elements like silica and alkalis in the oxide melts could be small. Compositions of the Fe-Ti  
220 oxides (Table 1) provide **no** chemical evidence for melting; the only elements present were those  
221 expected for crystalline oxide phases (Fe, Ti, Mg, Mn, Al, O). Even in experiments with added  
222 phosphate, there was no detectable P in the quenched oxides, nor was there any evidence for  
223 concentration of P and other “lithophile” elements around the perimeter of the oxide grains as  
224 might be expected if the oxide melt had successfully purged itself of those elements as it  
225 crystallized during quench. Thus if the oxides in Epler’s experiments had been immiscible  
226 melts, *phosphorus did not serve as an important flux* in forming them. All phosphorus -  
227 whether initially present in the rock samples or added as apatite or as  $(\text{Fe}_3(\text{P}_2\text{O}_7)_3)$  - was  
228 concentrated in the silicate melts that coexisted with the oxides (Table 2).

229  
230 Based on optical microscopy and backscattered electron imaging, the oxide phases  
231 appeared to be single-phase spinels. Epler’s electron microprobe analyses (which report all Fe  
232 as  $\text{FeO}^{\text{T}}$  since he was unable to analyze directly for oxygen) would be consistent with this  
233 interpretation if 10 to 20% of the iron present were ferric iron. Neither Epler nor his advisor  
234 were concerned about this apparent fact at the time, but in retrospect it should have raised our  
235 suspicions, because it is highly unlikely that an immiscible oxide melt would have spinel  
236 stoichiometry. For example, in his study of melting in the FeO-Fe<sub>2</sub>O<sub>3</sub>-TiO<sub>2</sub> system, Taylor  
237 (1963) showed maximum temperatures along the magnetite-ulvospinel join, with lower  
238 temperature cotectics on both the higher FeO and higher TiO<sub>2</sub> sides of that join. One would  
239 expect that behavior to persist in more complex systems, and while it is statistically possible for  
240 an immiscible oxide melt to have spinel stoichiometry, it is extremely unlikely that a series of



241 melts at different temperatures and from different starting compositions would all do so, an idea  
242 that will be revisited later in this review. Epler's M.S thesis was enthusiastically accepted in  
243 1987, and he moved on to other interests.

244

245

## NEW EXPERIMENTS

246

247

248

249

250

251

252

253

254

### **Attempts to prove melting by density difference**

255

256

257

258

259

260

261

262

263

264

265

266

267

268

269

### **Experiments on a different sample**

270

271           Next came experiments on a natural sample (GM123) from Iron Mountain, Wyoming. It  
272 is mainly oxide (titaniferous magnetite, ilmenite, and green spinel) plus olivine; pyroxene and  
273 plagioclase are virtually absent(<1% each). As in the Pt-ball experiments, the capsules were  
274 platinum-jacketed graphite, which had the advantages of forcing graphite saturation on the  
275 sample and eliminating the need to pre-soak Pt capsules with Fe. As with Epler's experiments,  
276 the textures were mainly ambiguous, with poorly-quenched silicate glass containing oxide grains  
277 that were mainly rounded, but that did show hints of euhedral faces. Once again there was the  
278 question: had the oxides been liquid droplets, developing partial faces either upon rapid  
279 crystallization during quench or possibly by quench overgrowth from the surrounding silicate  
280 melt? Or had they remained unmelted, but for some reason mainly failed to develop euhedral  
281 faces during the course of the experiment?

282  
283           One experiment (GM123-14), though, was especially enlightening. Natural fluorapatite  
284 (5.25 wt %) had been added to GM123 powder, so that if carbon, phosphate, or fluorine could  
285 flux oxide liquid, there was a good chance of producing an oxide melt. Pressure was 0.5 GPa,  
286 and the temperature was 1308°C - admittedly high in terms of expected natural conditions, but  
287 by this stage DHL was desperate to produce an unequivocal Ti- rich oxide melt! The run  
288 products were poorly-quenched silicate glass, Fo<sub>63</sub> olivine, and two oxide phases of distinctly  
289 different appearance and grain size. The coarser, dominant oxide phase (40-50 μm) was  
290 strongly reminiscent of those in Epler's experiments: partly rounded, partly euhedral, and with  
291 ~25 wt% TiO<sub>2</sub>. It also had a brownish reflectivity similar to that of Fe<sub>2</sub>TiO<sub>4</sub>-rich  
292 magnetite-ulvospinel solid solutions. The second phase was much smaller (~3-10 μm), lacked  
293 the brown tint, and had a higher FeO<sup>T</sup> and a much lower TiO<sub>2</sub> content (~3.3 wt. %; Table 3). Its  
294 texture was also ambiguous, ranging from rounded to subhedral. But importantly, its contents  
295 of SiO<sub>2</sub> (~0.8 wt%) and P<sub>2</sub>O<sub>5</sub> (~0.08 wt %), while low, were distinctly higher than in the larger  
296 oxide grains. Did it represent a small amount of immiscible (but low-Ti) oxide liquid?! And if  
297 so, were the larger oxide grains spinel crystals that had coexisted with both silicate and FeO-rich  
298 liquids? Even if the FeO-rich oxide did represent a melt, its low TiO<sub>2</sub> content strongly suggests  
299 that such a melt could not be parental to TiO<sub>2</sub>-rich oxides in nature. It also seemed possible that  
300 it might be a crystalline wüstite phase rather than a melt. Taylor (1964) showed that at 1300°C

301 wüstite can coexist with Fe<sub>2</sub>TiO<sub>4</sub>-rich magnetite-ulvospinel solid solutions at log fO<sub>2</sub> values from  
302 ~-8.5 to -10.5 - a range broadly consistent with graphite saturation at 0.5 GPa.

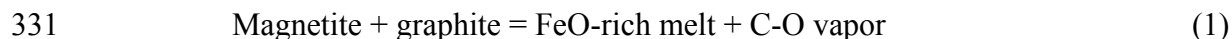
303  
304 Those questions were partly answered in 1992 when the Stony Brook electron  
305 microprobe was equipped with a detector crystal that permitted direct determination of oxygen.  
306 Re-analysis of larger oxide grains in GM123-14 showed 2.968 to 3.004 (average 2.992) cations  
307 per 4 oxygens - essentially perfect spinel stoichiometry (Table 3)! **This led to the conclusion**  
308 **that they had been crystalline spinels - not immiscible melt droplets - at the temperature of**  
309 **the experiment.** And since Epler's experiments were all performed at lower temperatures and  
310 produced similar textures and compositions, it seemed likely that the oxides in his experiments  
311 were also crystals rather than immiscible oxide melts, a conclusion further bolstered by the  
312 platinum-ball experiments described above. The new measurements on the low-TiO<sub>2</sub> oxide  
313 phase gave 0.88 cations per oxygen, slightly lower than the usual range for pure wüstites  
314 (0.90-0.95). Because of its relatively high contents of components like SiO<sub>2</sub>, TiO<sub>2</sub>, and Al<sub>2</sub>O<sub>3</sub>  
315 (total 4-5 wt. %), it is interpreted as having been a melt rather than a crystalline wüstite phase.  
316 And if it was a melt, its low P<sub>2</sub>O<sub>5</sub> content (0.08 wt.%) suggests that it was mainly fluxed by  
317 carbon rather than by the apatite added to this experiment.

318  
319 **Repeating Weidner's Fe-C-O experiments; adding TiO<sub>2</sub> and then phosphate**

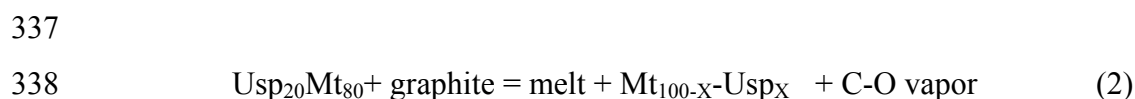
320  
321 Because the only likely melts in our experiments to date were FeO-rich and TiO<sub>2</sub>-poor,  
322 DHL decided to return to the simple system Fe-C-O, repeating Weidner's (1982) experiments  
323 but at 0.5 GPa. The experimental set-up was similar to that for sample GM123 (above). Even  
324 in that simple system, the presence of melt has to be inferred from textures, because it quenches  
325 to a wüstite-like oxide, never a glass. Weidner described in detail the textural features he  
326 interpreted as indicating oxide melt: "the quench liquids are ...vesiculated...and generally possess  
327 a meniscus" (1982, p. 559).

328  
329 Lindsley and Philipp (1993) bracketed the reaction

330



332  
333 between 1025 and 1050°C at 0.5 Gpa, in good agreement with Weidner's data at lower pressures.  
334 Having convinced ourselves that we could recognize iron-oxide melt in this simple system, we  
335 next added TiO<sub>2</sub> by replacing the pure magnetite with ulvospinel<sub>20</sub>-magnetite<sub>80</sub> leading to the  
336 reaction:



339  
340 where the proportion of melt and the value of X both increased with temperature: X  $\cong$  31  
341 (1075°C); X  $\cong$  37 (1100°C); and X  $\cong$  52 (1150°C). These samples were not microprobed; the  
342 composition of the product spinel was estimated from its XRD patterns. From mass balance, we  
343 concluded that the melt probably contained very little TiO<sub>2</sub>.

344  
345 The next step was to add apatite (or Fe<sub>3</sub>(P<sub>2</sub>O<sub>7</sub>)<sub>3</sub>) to test whether phosphate might increase  
346 the solubility of Ti in the melt. The most informative of this set of experiments was that named  
347 Usp70GrAp(4). The starting material was a mixture of 79 wt.% synthetic Usp<sub>70</sub>-Mt<sub>30</sub>, 4%  
348 graphite, and 17% natural apatite (Durango); this was run at 0.5 GPa, 1250°C for 19 hours.  
349 Products were two oxides (the more abundant one was brownish in reflected light, the less  
350 abundant one tended to be bright and interstitial), graphite, and apatite (Fig. 3A). XRD of the  
351 product showed ~70 wt. % spinel (~Usp<sub>77</sub> Mt<sub>23</sub>); ~28% apatite; ~2% wüstite; plus a small  
352 amount of graphite. The increase in the Ti content of the spinel is consistent with the notion  
353 that it is mainly the Fe<sub>3</sub>O<sub>4</sub> component that is reduced and enters any melt, with the bulk of the  
354 spinel remaining crystalline; that melt would quench mainly to wüstite. An alternative  
355 possibility is that the Fe<sub>3</sub>O<sub>4</sub> component was directly reduced to wüstite, with no melting taking  
356 place. However, semi-quantitative energy-dispersive analysis of the interstitial wüstite-like  
357 phase shows 95 wt. % FeO<sup>T</sup>; 4% TiO<sub>2</sub>; 0.5 % each of CaO and SiO<sub>2</sub>, and possibly 0.1 % P<sub>2</sub>O<sub>5</sub>  
358 (although that value must be very close to the detection limit; see Fig. 3B). It appears that the  
359 interstitial oxide phase dissolved more Ca than P from the apatite. Its TiO<sub>2</sub> content seems

360 suspiciously high had that phase never been melted, but the solubility of  $\text{TiO}_2$  in crystalline  
361 wüstite is not well known (see, for example, MacChesney and Muan, 1961). The  $\text{SiO}_2$  content -  
362 which appears to be real - is intriguing because the experiment was nominally silica-free! Silica  
363 may have been introduced along with the natural apatite (Durango apatite occurs with quartz), or  
364 the source may have been the agate mortar used to homogenize the starting mix. Whatever the  
365 source, it is tempting to conclude that the trace of silica present was concentrated in the small  
366 amount of wüstite-like melt that formed during the experiment.

367  
368 The presence of two oxide phases - one Ti-rich, the other Ti-poor in the quench products  
369 of experiments like GM123-14 and  $\text{Usp}_{70}\text{GrAp}(4)$  places important limits on interpretations of  
370 melting. There are three possibilities; the oxides represent: (1) Two immiscible oxide melts; (2)  
371 Two crystalline oxides; (3) One melt, one crystalline oxide. Case (1) seems unlikely; far from  
372 there being two coexisting melts in the pure Fe-Ti-O system at one atmosphere, there is a distinct  
373 **cotectic** between wüstite and the magnetite-ulvospinel join (Taylor, 1964), and there is no reason  
374 to suspect that elevated pressure or (relatively minor) addition of other components would so  
375 greatly change that behavior. Case (2) is not falsified by the available data - but it would mean  
376 that NO oxide melts were produced in these experiments - both of which were at temperatures  
377 higher than any of Epler's. That would mean there is **no** experimental evidence for the  
378 existence of Fe-Ti-oxide melts at and even above geologically plausible temperatures.

379  
380 Thus case (3) is probably correct, and if so the much more likely melt candidate is the  
381 Ti-poor phase. First, the distinctly more abundant Ti-rich oxide in GM123-14 has spinel  
382 stoichiometry (Table 3) (this was later confirmed by microprobe analysis for  $\text{Usp}_{70}\text{GrAp}(4)$  as  
383 well, see below), which is most unlikely for a melt. Second, had it been a melt, it would  
384 probably have dissolved the rather small proportion of the wüstite-like, low-Ti phase, becoming  
385 displaced from the spinel join towards the wüstite-spinel cotectic and thereby losing spinel  
386 stoichiometry! Third, the Ti-rich phase has very low contents of "non-spinel" components like  
387 silica,  $\text{P}_2\text{O}_5$ , and CaO - components expected to be present in an oxide melt that coexisted  
388 stably with a silicate melt. In contrast, the wüstite-like phase departs from probable wüstite  
389 composition. It contains 3-4 wt. % of  $\text{TiO}_2$ , probably greater than the solubility of  $\text{TiO}_2$  in

390 crystalline wüstite (MacChesney and Muan, 1961). Its contents of  $\text{SiO}_2$  and  $\text{P}_2\text{O}_5$ , while low,  
391 are nevertheless distinctly higher than those in the high-Ti phase. Finally, formation of a  
392 wüstite-like melt would be quite compatible with the findings of Weidner (1982) in the Ti-free,  
393 but C-bearing system. For all these reasons we conclude that if *any* Fe-oxide-rich melt was  
394 produced in all our experiments, it quenched to the relatively minor, low-Ti, FeO-rich  
395 wüstite-like phase seen in experiments GM123-14 and  $\text{Usp}_{70}\text{GrAp}(4)$ . Such a melt probably  
396 would not have formed as a separate phase in Epler's experiments, for it would have been  
397 dissolved into the abundant silicate melts present.

398  
399 **New electron microprobe data.** Symmes' 1992 analyses of sample GM123-14 show  
400 that the high-Ti oxide phase has spinel stoichiometry, and it plots on a temperature maximum  
401 (Fig. 4) when projected onto Taylor's melting diagram (1963). While it is therefore unlikely to  
402 represent a melt composition, it is possible for an exceptional case to have done so. As a final  
403 check, we decided to re-analyze some of Epler's "oxide melts" (as interpreted from textures) for  
404 oxygen to determine whether they might also have spinel stoichiometry. Accordingly, we  
405 selected samples from a range of temperatures (1100, 1150, and 1200°C) and starting materials  
406 (reduced and unreduced ORT; ORE) among Epler's experiments. We also analyzed sample  
407  $\text{Usp}_{70}\text{GrAp}-4$  and re-analyzed the Ti-rich phase of GM123-14 as a check. The results (Table  
408 5) are all consistent with the oxide phases being essentially stoichiometric spinels, and as such  
409 plot on or near a thermal maximum in the  $\text{FeO}-\text{Fe}_2\text{O}_3-\text{TiO}_2$  system (Fig. 5). We consider it most  
410 unlikely that they can represent quenched oxide melts - despite the textures we had originally  
411 interpreted as indicating melting.

412  
413 Several things are worth noting. By far the greatest uncertainty in the analyses (Table 4)  
414 is in the measurement of oxygen, as shown by the large standard deviations for that element and  
415 also for FeO and  $\text{Fe}_2\text{O}_3$ , which are of course calculated using the oxygen values. The  
416 re-analysis for oxygen of GM123-14 barely overlaps (at the one-sigma level) with that of 1992  
417 (Table 3; Fig. 4), further illustrating the difficulties in obtaining accurate analyses for oxygen.  
418 The results for experiment  $\text{Usp}_{70}\text{GrAp}-4$  were initially surprising, as the oxide phase plots near  
419  $\text{Usp}_{70}\text{Mt}_{30}$  - essentially unchanged from the composition of the starting oxide (XRD had

420 suggested that it had changed  $\sim\text{Usp}_{77}\text{Mt}_{23}$ ). But XRD also suggested that the amount of the  
421 wüstite-like probable melt phase was only  $\sim 2\%$ , and it seems possible that the microprobe  
422 analyses concentrated on mainly unreacted cores of zoned crystals, whereas the XRD would be  
423 mainly representative of reacted rims. It may be significant that  $\text{Usp}_{70}\text{GrAp-4}$  is the only one of  
424 these experiments that lacked a coexisting silicate-melt phase - possibly those melts facilitated  
425 reaction rates in the other experiments.

426  
427 One reviewer suggested that possibly the duration of our experiments was too short to  
428 produce oxide melt, but we consider this unlikely. First, the silicates did melt, and dissolved  
429 considerable portions of the oxides in the process. Second, the oxides produced in Epler's  
430 experiments **grew** in size (they were at least twice as large as the grains in the starting material)  
431 and thus had every opportunity to melt if oxide melt were the stable phase.

432

433

#### IMPLICATIONS

434

435 Despite all the efforts described above, we have found no good experimental evidence for  
436 the existence of *Ti-rich* Fe-Ti-oxide melts at geologically plausible temperatures. Addition of  
437 the fluxes proposed in the literature - apatite (phosphate; possibly fluorine) and carbon - failed to  
438 induce melting. Our conclusions are bolstered by the recent work of Wang et al. (2017), who  
439 successfully melted a mixture of one-third apatite, two-thirds Fe-Ti oxides at  $1450^\circ\text{C}$  and one  
440 atm. (thus even higher than Philpott's experiments!), but were unable to melt it at  $1200^\circ\text{C}$  and  
441  $0.3\text{ GPa}$ , even in the presence a vapor consisting of  $8\%\text{ H}_2\text{O}$  and  $8\%\text{ F}$ . Thus neither of those  
442 volatiles served as a flux. It remains possible that there exists a completely unanticipated flux  
443 that stabilizes such melts, but until experimental evidence confirms such a *fluxus ex machina*, we  
444 conclude that high-Ti oxide melts do not exist in nature. How then do we explain the dike-like,  
445 apparently intrusive Fe-Ti oxide bodies so typical of anorthosite suites? We suggest that the  
446 answer lies partly in the *silicate* liquids produced in Epler's experiments (Table 2). Those  
447 liquids contain large amounts of normative magnetite and ilmenite, and clearly were in  
448 equilibrium with Fe-Ti oxides very similar to those found in nature. Furthermore, their  
449 compositions are broadly similar to some members of the anorthosite suite that are variously

450 called jotunitites, ferrodiorites, and oxide-rich ferrodiorites, and that typically cross-cut massif  
451 anorthosites and are considered by many to represent magmas residual to the anorthosites  
452 themselves (for example, Mitchell, et al., 1996, their Table 2; Scoates et al., 2010, their Fig.16).  
453 One striking example is shown in Fig. 6, which compares the compositions of Epler's melt 64T  
454 at 1100°C (see table 2) and that of a monzodiorite dike found near the Sybille Pit oxide deposit  
455 in the Laramie Anorthosite Complex (Fuhrman, 1986). We suggest that many of these dikes  
456 represent melts that are residual to *both* the anorthositic rocks *and* the associated oxide deposits.  
457 Importantly, Epler's experiments show that such melts can exist at plausible temperatures,  
458 despite their typically low SiO<sub>2</sub> content.

459

460 We must be careful not to over-interpret the significance of the compositions of those  
461 melts (since Epler's experiments were only designed to search for oxide melts), but it appears  
462 that increasing contents of P<sub>2</sub>O<sub>5</sub> lead to increases in the solubility of both FeO<sup>T</sup> and TiO<sub>2</sub> in the  
463 silicate melts (Table 2). Green and Watson (1982) and Tollari et al. (2006) show that SiO<sub>2</sub> and  
464 P<sub>2</sub>O<sub>5</sub> vary antithetically in apatite-saturated silicate melts of a variety of compositions. Direct  
465 comparisons between their results and Epler's are difficult: while many of the Tollari et al. melts  
466 were saturated with Fe-Ti oxides *and* apatite, the experiments were conducted at 1 atm only. In  
467 contrast, Green and Watson's apatite-saturated experiments include pressures comparable to  
468 Epler's, but few if any were also saturated with Fe-Ti oxides. Only one of Epler's melts was  
469 apatite-saturated (64T, 1100°C), but all coexisted with Fe-Ti oxides. While the underlying  
470 mechanisms are unclear, it appears that low SiO<sub>2</sub> contents of silicate melts are commonly  
471 associated with unusually high concentrations of FeO<sup>T</sup>, TiO<sub>2</sub>, and P<sub>2</sub>O<sub>5</sub> (partly, of course, this is  
472 simply a zero-sum effect, but it appears to be more than that.) Does a lower silica content  
473 caused by higher P<sub>2</sub>O<sub>5</sub> simply allow greater solubilities of iron and titanium? Do increasing  
474 amounts of FeO<sup>T</sup> (and perhaps TiO<sub>2</sub>) and P<sub>2</sub>O<sub>5</sub> mutually enhance their solubilities in silicate  
475 melts? That would be intriguing, for it would mean that as a magma became saturated in, say,  
476 apatite, it would quickly become saturated in Fe-Ti oxides as well - and *vice versa*. That  
477 co-precipitation could help explain why oxide bodies are so often associated with abundant  
478 apatite - without any need to invoke a "nelsonite eutectic". Whatever the mechanism, it seems  
479 clear that the Fe-Ti oxide bodies formed from *silicate* melts rich in Fe, Ti, and P. Namur et al.



480 (2012) among others have suggested that Fe-Ti oxide bodies may have formed through fractional  
481 crystallization from the more mafic, silica-poor of two immiscible silicate melts. This is  
482 certainly possible, since studies of silicate liquid immiscibility show that Fe, Ti, and P are all  
483 concentrated in the conjugate melt having lower SiO<sub>2</sub> (for example, Naslund, 1983; Watson,  
484 1976). However, it is not *necessary* to invoke silicate liquid immiscibility; Scoates and  
485 Lindsley (2000) and Whitaker et al (2007a,b) have shown that basaltic melts can evolve directly  
486 to low-silica residua enriched in Fe, Ti, and P at pressures near 1 GPa. Such pressures are  
487 probably high for the *emplacement* of anorthosite suites within the crust, but may well reflect the  
488 conditions under which the plagioclase originally accumulated near the crust-mantle boundary,  
489 as proposed in the two-stage model for anorthosite genesis (Morse, 1968; Emslie, 1985; Longhi  
490 and Ashwal, 1985).

491  
492 If we accept that Fe-Ti oxide bodies were never liquid, but instead accumulated as  
493 crystals from Fe- and Ti-rich silicate melts (probably residual to anorthosites), how do we  
494 explain the strong field evidence that the oxide bodies cross-cut older rocks - including in many  
495 cases anorthosites themselves? It seems clear that the oxides were mobile in some fashion. We  
496 suggest two mechanisms. (1) The oxide cumulate may have been lubricated by a small amount  
497 of residual silicate liquid, most or all of which was squeezed out during emplacement. That  
498 squeeze-out would be represented by some of the “jotunitic” dikes so commonly associated with  
499 anorthosite complexes. (2) In many cases, the original oxide may have been mainly or entirely  
500 spinel, as suggested by Bolsover (1986) (and as supported by Epler’s experiments (1987)) and  
501 by Pang et al. (2008). Yet commonly the oxide bodies also contain varying amounts of  
502 ilmenite, both as separate grains and as lamellae within Fe<sub>3</sub>O<sub>4</sub>-rich spinel. Buddington and  
503 Lindsley (1964) suggested that both types of ilmenite can form from oxidation of Fe<sub>2</sub>TiO<sub>4</sub>  
504 component within the original spinel. At higher temperatures (say, >900°C) the ilmenite  
505 migrates to form separate grains (the granule oxy-“exsolution” of Buddington and Lindsley), and  
506 we suggest that the oxide mass will be quite weak during this recrystallization process and able  
507 to flow readily. Indeed, deformation during flow may also aid in the separation of the oxide  
508 phases. We suggest that these two mechanisms may yield sufficient mobility to permit the  
509 oxides to cross-cut the host rocks - presumably intruding downward because of their greater

510 density (e.g., Saint-Urbain Fe-Ti oxide deposit, Morisset et al., 2010). Till and Moscovitz  
511 (2013) summarize available data on the deformation of magnetite. Even though the experiments  
512 were on pure Fe<sub>3</sub>O<sub>4</sub> and were performed at lower temperatures than seem likely for granule  
513 oxy-“exsolution” of ilmenite from Fe-Ti spinel, they do show that magnetite is considerably  
514 weaker than plagioclase at a given T. Thus their study bolsters our suggestion that the (mainly  
515 crystalline) oxide accumulations were sufficiently weak to flow at high-subsolidus temperatures.

516  
517 Why, then, do the oxides in many of our experiments show textures (rounded outlines)  
518 suggesting they had been melts? One possibility is suggested by silicate melting experiments  
519 done in iron capsules. By definition, the melts are saturated with metallic iron, and the melts  
520 typically have inclusions of iron. Those inclusions typically are rounded globules, suggesting  
521 texturally that they were immiscible droplets of iron melt suspended in the silicate! Yet the iron  
522 capsules themselves do not melt, showing that the temperature of the experiment was clearly  
523 below the melting point of iron metal. Either the globules had dissolved some unknown and  
524 undetectable flux, or they were crystals of iron having rounded surfaces. One experiment  
525 conducted by DHL was particularly instructive. It was performed in an incompletely filled iron  
526 capsule within an evacuated silica-glass tube, and a meniscus formed at the top of the silicate  
527 melt. Metallic iron particles completely within the melt had rounded outlines, while those at the  
528 meniscus *were rounded where in contact with the melt but had beautiful euhedral faces where in*  
529 *contact with the (tenuous) vapor phase!* It seems clear that the iron was crystalline but that  
530 contact with the melt inhibited formation of euhedral faces, presumably through a surface-energy  
531 effect. We suggest that there may have been a similar effect on the oxides in our experiments.

532  
533 We realize that our experiments do not bear directly on the origin of ilmenite-rich oxide  
534 bodies such as those occurring in southeastern Canada, the Adirondacks, and the type nelsonites  
535 of Nelson County, Virginia. Those bodies generally have much higher Ti:Fe than those of this  
536 study, and their oxygen content is higher (typically the oxides are hemoilmenites with ~ 30%  
537 Fe<sub>2</sub>O<sub>3</sub>). And they are typically associated with andesine (K-rich feldspar in the unique case at  
538 Nelson County) rather than labradorite anorthosites, so there are clearly important differences  
539 relative to the rocks we have studied. Nevertheless, despite those differences, the

540 commonalities strongly suggest a broadly similar origin - for example, variations within the  
541 general outlines of the two-stage model (Morse, 1968; Emslie, 1985; Longhi and Ashwal, 1985)  
542 generally accepted for Proterozoic anorthosites. Explaining those differences is beyond the  
543 scope of this study, but one possibility is that the andesine anorthosite kindred may have  
544 assimilated more crustal material than have the labradorite anorthosites. For example, Frost et  
545 al. (2010) showed that the Snow Creek Anorthosite has assimilated more crustal material and has  
546 higher silica activity and  $fO_2$  than the other plutons of the Laramie Anorthosite Complex in  
547 Wyoming; the dominant Fe-Ti oxide mineral in the Snow Creek is ilmenite or hemoilmenite,  
548 whereas the other anorthosites have mainly spinel. Whatever the reason for the differences,  
549 however, there remains no experimental evidence that the ilmenite-rich bodies were ever oxide  
550 melts.

551  
552 Our experiments do support Weidner's finding (1982) that the presence of carbon greatly  
553 increases the stability of *Ti-poor* iron oxide melts - down into the "geologically plausible" range.  
554 If the Ti-poor "magnetite lava flows" at El Laco, Chile (Park, 1961; Naslund et al. 2002) ,  
555 actually formed from an iron oxide magma (and this interpretation is hotly debated), the effects  
556 of carbon surely help provide an explanation for the existence of such melts - if not for the actual  
557 mechanism by which they have formed. Likewise, the Ti-poor "high iron melts" reported by  
558 Hurai et al. (1998) could also have been stabilized by carbon; those authors report abundant  $CO_2$ ,  
559 both as bubbles in inclusions and dissolved in accompanying glass. However, if the two  
560 high-Ti (24%  $SiO_2$ , 43.9%  $TiO_2$ , and only 10.6 %  $FeO^T$ ) globules reported by Hurai et al. were  
561 really melts, they are clearly something very new and unusual and deserve further study.

562 Perhaps the strongest evidence to date for the possible existence of very low-Si and  
563 Fe-Ti-rich melts comes from Kamenetsky et al. (2013), who reported droplets of silica-rich melt  
564 coexisting with droplets of silica-poor melt ( $SiO_2$ , 15–46; FeO, 15–22;  $TiO_2$ , 2–7; CaO, 11–27;  
565  $P_2O_5$ , 5–30; wt. %) in a Siberian trap. However, these unusual compositions are most likely an  
566 anomaly, as they occur as millimeter-sized inclusions formed *within metallic iron droplets* where  
567 the trap encountered a coal seam, and thus at many orders of magnitude lower in  $fO_2$  than for the  
568 rocks being considered here.

569

570 One of our reviewers noted that we had not considered the possible effect of water as a  
571 flux to stabilize Fe-Ti oxide melts, citing the work of Lester et al. (2013), who reported forming  
572 an immiscible melt having 72.8% FeO<sup>T</sup> and only 7.14% SiO<sub>2</sub> at 1075°C in the presence of a  
573 water-rich vapor. But that melt contains 16.6% sulfur, and *no* TiO<sub>2</sub>, and thus is very different  
574 from the materials being considered here. Furthermore, there is compelling evidence that the  
575 orebodies and anorthosites in the Laramie Anorthosite Complex, at least, were strikingly dry.  
576 For the Sybille Pit, for example, Bolsover (1986) reported typically 0-3% “secondaries” that  
577 include biotite (Ti-rich and thus likely to be H<sub>2</sub>O-poor), amphibole, and prehnite, even in  
578 samples that contain up to 35% silicates. But perhaps the most compelling argument for very  
579 dry conditions within the LAC is the first author’s observation that, where water-rich granitic  
580 dikes cut the anorthositic rocks, those rocks are extensively altered for a distance of up to *ten*  
581 *times* the dike’s thickness on either side: the dark gray to black plagioclase is bleached white,  
582 and the ferromagnesian minerals are largely converted to dark-green amphibole! Quite clearly  
583 the anorthositic rocks had seen very little water prior to intrusion of the granitic dike. The  
584 presence of graphite within the LAC orebodies (Eberle, 1983; Bolsover, 1985; Epler, 1987) and  
585 abundant “plumbago” deposits within and surrounding the LAC strongly suggests that any vapor  
586 originally present was rich in C-O rather than H<sub>2</sub>O.

587

588

589

## CONCLUSIONS

590

591 1. At present there is no plausible experimental evidence for the existence of Ti-rich Fe-Ti  
592 oxide melts at geologically reasonable temperatures. Neither apatite nor carbon are effective  
593 fluxes, although both have been proposed as the way such liquids could be stabilized. We  
594 conclude that cross-cutting oxide “dikes” were probably emplaced in the solid state, possibly  
595 lubricated by small amounts of residual silicate melt, and by recrystallization accompanying  
596 granule oxy-“exsolution” of ilmenite from Fe<sub>2</sub>TiO<sub>4</sub>-rich spinel.

597

598 2. Although our experimental data are not conclusive, we suggest that increasing contents of  
599 P<sub>2</sub>O<sub>5</sub> and FeO (and possibly TiO<sub>2</sub>) mutually enhance their solubility in *silicate* melts, allowing

600 those components to build up in melts residual to anorthosites. Once those melts become  
601 saturated with either apatite or a Fe-Ti oxide phase, the other phase will also crystallize, thereby  
602 explaining why varying amounts of apatite typically accompany Fe-Ti oxide orebodies.

603  
604 3. We suggest that at least some of the “jotunitic” (low-Si, high-Fe and Ti) dikes associated  
605 with anorthosite suites may be doubly residual: residual first to nearby anorthosite, and second  
606 following the gravitational separation of crystalline Fe-Ti oxides that accumulated into the  
607 distinctive oxide bodies typically associated with anorthosites. Epler’s experiments produced  
608 silicate liquids (similar in composition to many of those dikes) at temperatures as low as 1100°C.

609  
610 4. We have great admiration and affection for Tony Philpotts, but we respectfully suggest that it  
611 is past time for workers to stop referring to his 1967 experiments - with their unreasonably high  
612 temperatures and near-absence of titanium - as evidence for the existence of Fe-Ti oxide magmas  
613 in nature. They simply are not!

614

615

616

#### ACKNOWLEDGMENTS

617

618 We thank Gregory Symmes, Susan Swapp, and Adrian Fiegl for help with electron  
619 microprobe analyses, and Jim Quinn for help with electron microscopy. Jon Philipp and Qiang  
620 Zeng worked on the Fe-C-O experiments with added components. The experiments reported  
621 here and earlier electron microprobe analyses were supported by a series of NSF grants to DHL  
622 in the 1980s and 1990s. Recent microprobe work at the American Museum of Natural History  
623 was supported by NSF Grant EAR1249696 to Hanna Nekvasil. The manuscript was improved  
624 through comments on an early version by Lew Ashwal, Tony Morse, and especially James  
625 Scoates, and on the submitted version by Bernard Charlier and Dick Naslund; we thank them all.

626

627

#### REFERENCES

628

629 Ashwal, L.D. (1978) Petrogenesis of massif-type anorthosites: crystallization history and liquid

- 630 line of descent of the Adirondack and Morin Complexes. Unpublished Ph.D. thesis,  
631 Princeton University, 136 p.  
632
- 633 Ashwal, L.D. (1993) Anorthosites. Springer-Verlag, Berlin, xix + 422 pp.  
634
- 635 Asklund, B. (1949) Apatitjärnmalmernas differentiation. Geologiska Föreningen Stockholm  
636 Förhandlingar, 71, 127-176  
637
- 638 Bai, Z.-J., Zhong, H., Li, C., Zhu, W.-G., and Hu, W.-J. (2016 - in press) Association of cumulus  
639 apatite with compositionally unusual olivine and plagioclase in the Taihe Fe-Ti oxide  
640 ore-bearing layered mafic-ultramafic intrusion: Petrogenetic significance and  
641 implications for ore genesis. American Mineralogist, 101, 2168-2175.  
642
- 643 Bateman, A.M. (1951) The formation of late-magmatic oxide ores. Economic Geology, 46,  
644 404-426.  
645
- 646 Bolsover, L.R. (1986) Petrogenesis of the Sybille iron-titanium oxide deposit. Laramie  
647 anorthosite complex, Laramie Mountains, Wyoming. Unpublished M.S. Thesis, State  
648 University of New York at Stony Brook, Stony Brook, NY, 78 p.  
649
- 650 Boyd, F.R. and England, J.L. (1963) Effect of pressure on the melting of diopside  $\text{CaMgSi}_2\text{O}_6$   
651 and albite  $\text{NaAlSi}_3\text{O}_8$  in the range up to 50 kilobars. Journal of Geophysical Research,  
652 68, 311-323.  
653
- 654 Buddington, A.F., Fahey, J, and Vlisidis, A. (1955) Thermometric and petrogenetic significance  
655 of titaniferous magnetite. American Journal of Science, 253, 497-532.  
656
- 657 Buddington, A.F. And Lindsley, D.H. (1964) Iron titanium oxide minerals and synthetic  
658 equivalents. Journal of Petrology, 5, 310-357.  
659

- 660 Charlier, B., Namur, O., Bolle, O. Latypov, R., and Duchesne, J.-C. (2015) Fe-Ti-V-P ore  
661 deposits associated with Proterozoic massif-type anorthosites and related rocks. Earth  
662 Science Reviews, 141, 56-81.  
663
- 664 Chen, H.-K., and Lindsley, D.H. (1983) Apollo 14 very low titanium glasses: Melting  
665 experiments in iron-platinum alloy capsules. Proceedings of the Fourteenth Lunar and  
666 Planetary Science Conference, Part 1, Journal of Geophysical Research, 88, supplement,  
667 B335-B342.  
668
- 669 Chung, S.L., and Jahn, B.M. (1995) Plume-lithosphere interaction in generation of the Emeishan  
670 flood basalts at the Permian-Triassic boundary. Geology, 23, 889-892.  
671
- 672 Darken, L.S., and Gurry, R.W. (1946) The system iron-oxygen. II. Equilibrium and  
673 thermodynamics of liquid oxide and other phases. Journal of the American Chemical  
674 Society, 68, 798-816.  
675
- 676 Duchesne, J.-C. (1996) Liquid ilmenite or liquids ilmenite: a comment on the nature of ilmenite  
677 vein deposits. In: Demaiffe, D.. (ed) Petrology and geochemistry of magmatic suites of  
678 rocks in the continental and oceanic crusts. A volume dedicated to Professor Jean  
679 Michot, Université Libre de Bruxelles, Royal Museum for Central Africa (Tervuren),  
680 73-82. [Not available to the authors, but cited in Duchesne (1999)]  
681
- 682 Duchesne, J.-C. (1999) Fe-Ti deposits in Rogaland anorthosites (South Norway): geochemical  
683 characteristics and problems of interpretation. Mineralium Deposita, 34, 182-198.  
684
- 685 Dymek, R.F., and Owens, B.E. (2001) Petrogenesis of apatite-rich rocks (nelsonites and  
686 oxide-apatite gabbroanorthosites) associated with massif anorthosites. Economic Geology,  
687 96, 797-815.  
688
- 689 Eberle, M.M.C. (1983) Genesis of the magnetite-ilmenite deposit at Iron Mountain, Laramie

- 690 Anorthosite Complex, Wyoming. Unpublished M. S. Thesis, University of Colorado,  
691 Boulder, x + 114 pp.
- 692
- 693 Emslie, R.F. (1975) Major rock units of the Morin Complex, southwestern Quebec.  
694 Geological Survey of Canada Paper 74-48, 37 p.
- 695
- 696 Emslie, R.F. (1985): Proterozoic anorthosite massifs. In A.C. Tobi, and J.L.R. Touret,, Eds. The  
697 Deep Proterozoic Crust in the North Atlantic Provinces, p. 39-60. D. Reidel Publishing  
698 Company, Dordrecht.
- 699
- 700 Epler, N.A. (1987) Experimental study of Fe-Ti oxide ores from the Sybille Pit in the Laramie  
701 anorthosite, Wyoming. Unpublished M. S. Thesis, Department of Earth and Space  
702 Sciences, State University of New York at Stony Brook, ix + 67 pp.
- 703
- 704 Frost, C.D., Frost, B.R., Lindsley, D.H., Chamberlain, K.R., Swapp, S M., and Scoates, J.S.  
705 (2010), Geochemical and isotopic evolution of the anorthositic plutons of the Laramie  
706 Anorthosite Complex: explanations for variations in silica activity and oxygen fugacity in  
707 anorthosites. Canadian Mineralogist, 48, 925-946
- 708
- 709 Fuhrman, M.L. (1986). Petrology and mineral chemistry of the Sybille monzosyenite and the  
710 role of ternary feldspars. Unpublished Ph.D. Dissertation, Department of Earth and Space  
711 Sciences, State University of New York at Stony Brook, x + 214 p.
- 712
- 713 Fuhrman, M.L., Frost, B.R., and Lindsley, D.H. (1988) Crystallization conditions of the Sybille  
714 Monzosyenite, Laramie Anorthosite Complex, Wyoming. Journal of Petrology, 29,  
715 699-729.
- 716
- 717 Green, T.H., and Watson, E.B. (1982) Crystallization of apatite in natural magmas under high  
718 pressure, hydrous conditions, with particular reference to 'Orogenic' rock series.  
719 Contributions to Mineralogy and Petrology, 93, 524-531.



- 720  
721 Gross, G.A. (1996) Mafic intrusion-hosted titanium-iron, in *Geology of Canadian Mineral*  
722 *Deposit Types*. O. R. Eckstrand, W. D. Sinclair and R. I. Thorpe, eds., Geological Survey  
723 of Canada, 8, 573-582.  
724  
725 Hargraves, R.B. (1962) Petrology of the Allard Lake anorthosite suite, Quebec. In: *Petrologic*  
726 *Studies, A Volume to Honor A. F. Buddington*. Geological Society of America, Denver,  
727 xii + 660 pp., p. 163-189.  
728  
729 Hurai, V., Simon, K., Wiechert, U., Hoefs, J, Konečnỳ, P., Huraiová, M., Pironon, J., and Lipka,  
730 J. (1998) Immiscible separation of metalliferous Fe/Ti-oxide melts from fractionating  
731 alkali basalt: *P-T-fO<sub>2</sub>* conditions and two-liquid elemental partitioning. *Contributions to*  
732 *Mineralogy and Petrology*, 133, 12-29.  
733  
734 Kamenetsky, V.S., Charlier, B., Zhitova, L., Sharygin, V., Davidson, P., and Fein, S. (2013)  
735 Magma-chamber-scale liquid immiscibility in the Siberian Traps represented by melt  
736 pools in native iron. *Geology*, 41, 1091-1094.  
737  
738 Kolker, A. (1982) Mineralogy and geochemistry of Fe-Ti oxide and apatite (nelsonite) deposits  
739 and evaluation of the liquid immiscibility hypothesis. *Economic Geology*, 77,  
740 1146-1158.  
741  
742 Lindsley, D.H., and Philipp, J.R. (1993) Experimental evaluation of Fe-Ti oxide magmas.  
743 *EOS*, 74, 337.  
744  
745 Lindsley, D.H. (2003) Do Fe-Ti oxide magmas exist? *Geology: Yes; Experiments: No!* In J.-C.  
746 Duchesne and A. Korneliussen, (eds.), *Ilmenite Deposits and Their Geological*  
747 *Environment: Norges Geologiske Undersøkelse Special Publication 9*, p. 34-35.  
748  
749 Lindsley, D.H., Frost, B.R., Frost, C.D., and Scoates, J.S. (2010) *Petrology, Geochemistry, and*

- 750 Structure of the Chugwater Anorthosite, Laramie Anorthosite Complex, S. E. Wyoming,  
751 USA., Canadian Mineralogist, 48, 887-923.  
752
- 753 Longhi, J. and Ashwal, L.D. (1985) Two-stage model for lunar and terrestrial anorthosites:  
754 Petrogenesis without a magma ocean. Proceedings of the 15th Lunar and Planetary  
755 Science Conference, Part 2. Journal of Geophysical Research, 90, suppl., C571-C584.  
756
- 757 MacChesney, J.B. and Muan, A. (1961) Phase equilibria at liquidus temperatures in the system  
758 iron oxide-titanium oxide at low oxygen pressures. American Mineralogist, 46, 572-582.  
759
- 760 Mitchell, J.M., Scoates, J.S., Frost, C.D., and Kolker, A. (1996). The geochemical  
761 evolution of anorthosite residual magmas in the Laramie Anorthosite Complex,  
762 Wyoming. Journal of Petrology, 37, 637-660.  
763
- 764 Morisset, C.-E., Scoates, J.S., Weis, D., Sauv e, M., and Stanaway, K.J. (2010) Rutile-bearing  
765 ilmenite deposits associated with the Proterozoic Saint-Urbain and Lac Allard anorthosite  
766 massifs, Grenville Province, Quebec. Canadian Mineralogist, 48, 821-849.  
767
- 768 Morse, S.A. (1968) Layered intrusions and anorthosite genesis. In Y. Isachsen, ed., Origin of  
769 Anorthosite and Related Rocks, New York State Museum and Science Service Memoir  
770 18, Albany, New York, p. 175-187  
771
- 772 Namur, O., Charlier, B., and Holness, M.B. (2012) Dual origin of Fe–Ti–P gabbros by  
773 immiscibility and fractional crystallization of evolved tholeiitic basalts in the Sept Iles  
774 layered intrusion. Lithos, 154, 100-114.  
775
- 776 Namur, O., Charlier, B., Toplis, M.J., Higgins, M.D., Li geois, J.-P., and Vander Auwera, J.  
777 (2010) Crystallization sequence and magma chamber processes in the ferrobasaltic Sept  
778 Iles layered intrusion, Canada. Journal of Petrology, 51, 1203-1236.  
779

- 780 Naslund, H.R. (1983) The effect of oxygen fugacity on liquid immiscibility in Fe-bearing silicate  
781 melts. American Journal of Science, 283, 1034-1059.  
782
- 783 Naslund, H.R., Henriquez, F., Nystrom, J.O., Vivallo, W., and Dobbs, F.M., 2002. Magmatic iron ores  
784 and associated mineralization: Examples from the Chilean high Andes and Coastal  
785 Cordillera, in T.M. Porter (ed.) Hydrothermal Iron Oxide Copper-Gold & Related  
786 Deposits: A Global Perspective, vol. 2, PGC Publishing, Adelaide, 207-226.  
787
- 788 Pang, K.-N., Zhou, M.-F., Lindsley, D., Zhao, D. and Malpas, J. (2008). Origin of Fe-Ti Oxide  
789 Ores in Mafic Intrusions: Evidence from the Panzihua Intrusion, SW China. Journal  
790 of Petrology 49(2), 295-313.  
791
- 792 Park, C.F. (1961) A magnetite “flow” in northern Chile. Economic Geology 56, 431–441.  
793
- 794 Philpotts, A.R. (1967) Origin of certain iron-titanium oxide and apatite rocks. Economic  
795 Geology, 62, 303-315.  
796
- 797 Reynolds, I. (1985) The nature and origin of titaniferous magnetite-rich layers in the Upper Zone  
798 of the Bushveld complex: a review and synthesis. Economic Geology, 80, 1089-1108.  
799
- 800 Scoates, J.S. and Lindsley, D.H. (2000). New insights from experiments on the origin of anorthosite.  
801 EOS, 81, F1300.  
802
- 803 Scoates, J.S., Lindsley, D.H, and Frost, B.R. (2010) Magmatic and structural evolution of an  
804 anorthositic magma chamber: the Poe Mountain intrusion, Laramie anorthosite complex,  
805 Wyoming (USA). Canadian Mineralogist, 48, 851-885.  
806
- 807 Taylor, R.W. (1963) Liquidus temperatures in the system FeO-Fe<sub>2</sub>O<sub>3</sub>-TiO<sub>2</sub>. Journal of the  
808 American Ceramic Society, 46, 276-279.  
809

- 810 Taylor, R.W. (1964). Phase equilibria in the system FeO-Fe<sub>2</sub>O<sub>3</sub>-TiO<sub>2</sub> at 1300°C. American  
811 Mineralogist, 49, 1016-1030.  
812
- 813 Till, J.L. and Moskowitz, B. (2013) Magnetite deformation mechanism maps for better  
814 prediction of strain partitioning. Geophysical Research Letters, 40, 697-702.  
815
- 816 Tollari, N., Toplis, M.J., and Barnes, S.J. (2006) Predicting phosphate saturation in silicate  
817 magmas: An experimental study of the effects of melt composition and temperature.  
818 Geochimica et Cosmochimica Acta, 70, 1518-1536.  
819
- 820 Wang, M., Veksler, I., Zhang, Z., Hou, T., and Keiding, J.K. (2017) The origin of nelsonite  
821 constrained by melting experiment and melt inclusions in apatite: The Damiao  
822 anorthosite complex, North China Craton. Gondwana Research, 42, 163-176.  
823
- 824 Watson, E.B. (1976) Two-liquid partition coefficients: experimental data and geochemical  
825 implications. Contributions to Mineralogy and Petrology, 56, 119-134.  
826
- 827 Watson, T.L. (1907) Mineral resources of Virginia: Lynchburg, Virginia. Jamestown Exposition  
828 Commission, 618 p.  
829
- 830 Weidner, J.R. (1982) Fe oxide magmas in the system Fe-C-O. Canadian Mineralogist, 20,  
831 555-566.  
832
- 833 Whitaker, M.L., Lindsley, D.H., Whitaker, J.M.K., and Nekvasil, H. (2007a) Carbon is not  
834 required during crystallization to produce ferrobasalts/ferrodiorites (FTP rocks).  
835 American Mineralogist, 92, 1750-1755.  
836
- 837 Whitaker, M.L., Nekvasil, H., Lindsley, D.H., and DiFrancesco, N.J. (2007b) The role of  
838 pressure in producing compositional diversity in intraplate basaltic magmas. Journal of  
839 Petrology, 48, 365-393.

840

841 Woodruff, L.G., Nicholson, S.W., and Fey, D.L., 2013, A deposit model for magmatic  
842 iron-titanium-oxide deposits related to Proterozoic massif anorthosite plutonic suites:  
843 U.S. Geological Survey Scientific Investigations Report 2010–5070-K, 47 p.,  
844 <http://pubs.usgs.gov/sir/2010/5070/k/>.

845

846 Young, E.J., Mayers, A.T., Munson, E.L., and Conklin, N.M. (1969) Mineralogy and  
847 geochemistry of fluorapatite from Cerro de Mercado, Mexico. U.S. Geological Survey,  
848 Professional Paper 650-D: 84-93.

849

850 Zhou, M.-F., Malpas, J., Song, X.-Y., Robinson, P.T., Sun, M., Kennedy, A.K., Leshner, C.M.,  
851 and Keays, R. R. (2002) A temporal link between the Emeishan large igneous province  
852 (SW China) and the end-Guadalupian mass extinction. Earth and Planetary Science  
853 Letters, 196, 113-122.

854

855

### Figure Captions

856

857 Fig. 1. Proportions (volume percent) of phases produced in Epler's melting experiments on ORT  
858 starting material (oxide-rich troctolite; Bolsover's sample SCP113). "T" indicates unreduced  
859 starting material; "TR" indicates starting material reduced at 1040°C and at  $fO_2$  "within the  
860 fayalite stability field". Components added: C, 4 wt. % synthetic carbon; "FeP", 5 wt. %  
861 ( $Fe_3(P_2O_7)_3$ ); "Ap" 7 wt. % natural apatite from Durango, Mexico. Numerals correlate with  
862 experiments listed in Table 1.

863

864 Fig. 2. Photomicrographs (reflected light) of Epler's experimental products (all at 0.5 GPa).  
865 A, Experiment 25T (unreduced ORT, 1200°C, 21.7 hours; 4 wt. % each of C and ( $Fe_3(P_2O_7)_3$ )  
866 added), showing typically ambiguous textures. Primary oxides (light) have both very rounded  
867 and euhedral boundaries with quenched silicate melt (medium gray with feathery quench oxides).  
868 We originally interpreted the textures to mean the oxides had been melts and that some euhedral  
869 faces formed during quench, both by rapid crystallization of the primary oxide and by

870 overgrowth of oxide components from the surrounding silicate melt. Dark gray, vesicles. B,  
871 Experiment 61T (ORE with added oxalic acid, 1200°C, duration not known). C, Experiment  
872 38T (unreduced ORT, 1150°C, 65.9 hours; 7 wt. % apatite added. Oxides (light gray) have  
873 both euhedral and rounded outlines; darker material, silicate glass with abundant feathery quench  
874 oxides; black, vesicles. D, Experiment 58D (ORE starting material at 1200°C, 65.8 hours, no  
875 added components). Both oxide grains (white) and poorly quenched silicate glass (darker with  
876 feathery quench oxides) conform to the shape of the central vesicle. Both Epler and his advisor  
877 considered this texture to be strong proof that the oxides were immiscible melts at the  
878 temperature of the experiment. E, Experiment 56D (ORE starting material at 1200°C, 4 wt. % C  
879 added; water may have diffused into the charge from intentionally undried furnace parts).  
880 Oxides (white) have ameboid outlines highly suggestive of melting. Darker gray is silicate  
881 glass with quench oxides. F, enlargement of E, showing that quench oxides in interstitial  
882 silicate glass are concentrated away from the primary oxides (large, white). Boundaries of the  
883 primary oxides are uneven, suggesting that oxide components from the adjacent melt nucleated  
884 on the primary oxides during quench. Scale bars are 50  $\mu\text{m}$ .

885 Fig. 3. Results for experiment  $\text{Usp}_{70}\text{GrAp}(4)$  (1250°C, 0.5 Gpa, 19 hours; see text). (A)  
886 Backscattered electron image of polished surface. Very light gray, Fe-rich, Ti-poor oxide - now  
887 mainly wüstite, but suspected of having been oxide melt (M); slightly darker gray, Ti-rich oxide,  
888 believed to have been crystalline spinel (Sp); medium gray, apatite (Ap); black, graphite (Gr).  
889 Accelerating voltage 20 kV. (B) energy-dispersive X-ray spectrum of suspected oxide melt  
890 pocket shown by small square in (A). Any F present (possibly contributed by the fluorapatite)  
891 is unfortunately masked by the Fe  $L\alpha$  peak near 0.7 keV.

892  
893 Fig. 4. Liquidus (melting) diagram for oxides in the system  $\text{FeO}-\text{Fe}_2\text{O}_3-\text{TiO}_2$  at one atm.  
894 (modified from Taylor, 1964). Heavy dash-double-dot line shows compositional range of  
895 stoichiometric spinels (magnetite-ulvospinel join) - a thermal maximum. Dash-single-dot line  
896 shows the extent of the wüstite field at the liquidus (Darken and Gurry, 1946). Temperatures  
897 drop off to cotectics (spinel-wüstite; spinel-rhombohedral phase) on either side of the spinel join.  
898 GM123-14 High Ti, the Ti-rich oxide produced from an olivine-oxide rock from Iron Mountain,  
899 Wyoming + 2% graphite + 5% apatite, 1308° C (see text for details). GM123-14 Low Ti is

900 interpreted as representing a likely oxide melt. Analyses (Table 3) by G. Symmes, Stony Brook  
901 microprobe in 1992. Size of symbols represents average of multiple analyses  $\pm$  one standard  
902 deviation. Projection scheme: "FeO" = FeO + MnO + MgO + CaO; "Fe<sub>2</sub>O<sub>3</sub>" = Fe<sub>2</sub>O<sub>3</sub> + Al<sub>2</sub>O<sub>3</sub> +  
903 trace P<sub>2</sub>O<sub>5</sub>; "TiO<sub>2</sub>" = TiO<sub>2</sub> + SiO<sub>2</sub>, all combined in *molar* proportions and then recalculated to  
904 *equivalent weight* percentages of FeO, Fe<sub>2</sub>O<sub>3</sub>, and TiO<sub>2</sub> to be compatible with Taylor's  
905 diagram.

906

907 Fig. 5. Enlargement of FeO-rich region of Fig. 4, showing projected compositions of oxides  
908 produced in attempted melting experiments, all at 5 GPa. Key: 54, 54T - oxide-rich troctolite  
909 (ORT; see Table 2) + 4% graphite, 1150° C. 37, 37TR - reduced ORT +7% apatite, 1150° C.  
910 38, 38T, ORT + 7% apatite, 1150° C. 39, 39T - ORT + 5% "FeP", 1150° C. 61, ORE (see  
911 Table 2) with oxalic acid, 1200° C. 45, 45T - ORT + 5% "FeP", 1100° C. 64, 64T - ORT + 7%  
912 apatite, 1100° C (all re-analyzed from Epler, 1987). U<sub>70</sub> - synthetic Usp<sub>70</sub>Mt<sub>30</sub>GrAp-4, 1250° C  
913 (see text for details). Usp<sub>50</sub>Mt<sub>50</sub> is a synthetic spinel used as a working standard for the  
914 analyses. All Ti-rich samples are consistent with representing single-phase spinels, not melts.  
915 All analyses include direct measurement of oxygen, and size of symbols represents average of  
916 multiple analyses  $\pm$  one standard deviation. GM123-14 (1992) and GM123-14 Low Ti, from  
917 Fig. 4; all others measured in 2016 at the American Museum of Natural History. Full analyses  
918 are given in Table 3 and Table 4. See caption for Fig. 4 for projection scheme.

919

920 Fig. 6. Log-log plot comparing compositions of Epler's silicate melt 64T (ORT with 7 wt. %  
921 apatite added; 1100°C, 0.5 GPa, 70.5 hours; see Table 2) and a monzodiorite dike close to the  
922 Sybille Pit oxide deposit, Laramie Anorthosite Complex (Table 1-7, p. 66, Fuhrman, 1986).  
923 Units in wt %. Diagonal line shows 1:1 correspondence.

924

925 Table 1. Compositions of Fe-Ti oxides in Epler's experiments - interpreted by him as being  
926 quenched melts immiscible with the silicate melts in Table 2.

927 Table 2. Compositions of starting bulk composition and of silicate melts produced in Epler's  
928 experiments.

929 Table 3. Compositions of silicate melt and oxide phases in experiment GM123-14

930 Table 4. Compositions of several Fe-Ti oxides (initially interpreted as quenched melts) in  
931 several experiments. All Ti-rich compositions approach spinel stoichiometry (3  
932 cations/4 oxygens.)



Table 1. Electron microprobe analyses of oxide phases in Epler's experiments (Epler, 1987, Tables 5-7)

Sample	42T	43T	47TR	48T	45T	64T	54T	39T	38T
Added comp.	none	none	none	4% C	5% "FeP"	7% Ap	4% C	5% "FeP"	7% Ap
Temp °C	1100	1100	1100	1100	1100	1100	1150	1150	1150
Duration (hrs.)	47.4	95.3	69.3	70.3	89.7	70.5	72.6	68.3	69.5
Wt %									
TiO <sub>2</sub>	22.30	21.10	25.90	25.40	22.60	22.70	29.90	27.00	28.40
Al <sub>2</sub> O <sub>3</sub>	5.42	5.10	6.41	6.74	5.22	5.62	5.51	5.41	5.13
FeO <sup>T</sup>	67.20	67.40	63.30	63.40	67.50	66.50	58.00	62.10	61.40
MgO	3.02	3.54	2.54	2.52	3.11	3.10	4.21	3.24	3.42
Total	97.94	97.14	98.15	98.06	98.43	97.92	97.62	97.75	98.35

Notes: ORT, Bolsover's oxide-rich troctolite SCP-113. xxT indicates experiments on unreduced ORT sta reduced at 1040°C and at fO<sub>2</sub> "within the fayalite stability field". FeO<sup>T</sup>, total iron expressed as FeO. Added components are: C, synthetic graphite. "FeP", synthetic Fe<sub>4</sub>(P<sub>2</sub>O<sub>7</sub>)<sub>3</sub>. Ap, fluorapatite. Si and P were searched for by energy-dispersive analysis and X-ray imaging, but not detected.

37TR 7% Ap	20TR none	22T 4% C	21TR 4% C	25T 4% C; 5% "FeP"	24TR 5% "FeP"	36TR 7% Ap
1150	1200	1200	1200	1200	1200	1200
70.2	26	27	21.8	21.7	30.6	47.2
29.00	26.70	27.20	29.00	29.10	29.10	29.20
5.61	6.32	6.84	6.34	7.50	6.01	5.63
60.30	60.50	59.40	58.30	61.20	58.90	57.60
3.83	4.03	4.04	4.24	3.73	3.60	5.81
98.74	97.55	97.48	97.88	101.53	97.61	98.24

ring material. xxTR indicates experiments on ORT that had been  
 d as FeO.

te from Durango, Mexico.

ected.

Table 2. Electron microprobe analyses of bulk rock and silicate melts<sup>a</sup> in Epler's experiments using ORT starting

Sample	SCP113	42T	43T	47TR	48T	45T	64T	54T	39T	38T
Added comp.	"LiB" <sup>b</sup>	none	none	none	4% C	5% "FeP"	7% Ap	4% C	5% "FeP"	7% Ap
Temp °C	1050	1100	1100	1100	1100	1100	1100	1150	1150	1150
Duration (hrs.)	0.5	47.4	95.3	69.3	70.3	89.7	70.5	72.6	68.3	69.5
Wt %										
SiO <sub>2</sub>	21.90	42.80	43.70	41.10	39.50	35.70	36.50	32.40	29.70	25.00
TiO <sub>2</sub>	14.00	4.04	4.43	3.30	3.56	4.30	4.17	7.79	6.21	8.56
Al <sub>2</sub> O <sub>3</sub>	8.65	11.87	11.90	13.00	12.00	9.75	9.98	10.40	8.79	8.74
FeO <sup>T</sup>	41.90	23.60	21.30	25.30	27.80	27.70	26.20	32.70	35.30	32.70
MnO	0.40	0.31	0.31	0.32	0.37	0.36	0.33	0.33	0.33	0.31
MgO	5.28	3.47	4.12	2.98	3.11	5.20	4.60	5.51	5.16	4.68
CaO	3.02	7.26	7.20	7.74	7.59	5.56	10.50	4.86	4.64	9.41
Na <sub>2</sub> O	1.31	2.17	2.44	2.79	2.47	1.94	2.05	1.80	1.77	1.34
K <sub>2</sub> O	0.24	0.60	0.61	0.59	0.49	0.44	0.47	0.39	0.35	0.27
P <sub>2</sub> O <sub>5</sub>	0.42	0.94	0.98	0.99	0.78	5.64	3.78	0.64	4.83	4.38
Total	97.00	97.06	96.99	98.11	97.67	96.59	98.58	96.82	97.08	95.39

Notes: ORT, Bolsover's oxide-rich troctolite SCP-113. xxT indicates experiments on unreduced ORT starting material reduced at 1040°C and at fO<sub>2</sub> "within the fayalite stability field". "LiB", 50% lithium metaborate and 50% boron oxide. C, synthetic graphite. "FeP", synthetic Fe<sub>4</sub>(P<sub>2</sub>O<sub>7</sub>)<sub>3</sub>. Ap, fluorapatite from Durango, Mexico.

<sup>a</sup>Melts produced at 1150 and 1200°C quenched to fine-grained intergrowths of silicate glass plus feathery quartz in an attempt to obtain representative melt compositions.

<sup>b</sup>Normalized to 97% to facilitate comparison to other analyses.

<sup>c</sup>Evidently Na and K were lost during either the experiment or the analysis.

g material (Epler, 1987, Tables 3-4)

37TR 7% Ap	20TR none	22T 4% C	21TR 4% C	25T 4% C; 5% "FeP"	24TR 5% "FeP"	36TR <sup>c</sup> 7% Ap
1150	1200	1200	1200	1200	1200	1200
70.2	26	27	21.8	21.7	30.6	47.2
27.10	31.30	30.80	31.30	26.10	26.20	20.00
7.63	8.64	7.03	8.89	10.40	9.51	13.20
8.74	11.80	8.88	10.00	9.43	9.38	11.60
31.20	35.20	37.20	35.50	36.70	38.20	32.10
0.33	0.37	0.37	0.39	0.36	0.41	0.34
4.56	4.97	5.29	5.23	4.88	5.15	4.45
10.30	4.30	4.42	4.71	3.87	4.08	7.37
1.27	1.29	1.78	1.71	1.34	1.61	0.94
0.34	0.30	0.37	0.39	0.30	0.32	0.22
4.91	0.54	0.63	0.63	3.52	2.78	3.59
96.38	98.71	96.77	98.75	96.90	97.64	93.81

aterial. xxTR indicates experiments on ORT that had been  
 dded as a flux to make a glass; reported bulk rock analysis

lexico. FeO<sup>T</sup>, total iron expressed as FeO.

h-formed oxides. Analyses used an enlarged beam

Table 3 Analyses of Experiment GM123-14 (0.5 GPa, 1308°C, 24 hours)

	Wyo(1990) <sup>a</sup>		Wyo(1990) <sup>a</sup>		SB (1992) <sup>c</sup>		AMNH (2016) <sup>e</sup>	
	Silicate melt		Large Oxides		Large Oxides		Large Oxides	
Wt. %	Avg of 2	Std Dev	Avg of 6	Std Dev	Avg of 9	Std Dev	Avg of 20	Std Dev
SiO <sub>2</sub>	30.161	0.211	0.20	0.10	0.15	0.01	0.15	0.02
TiO <sub>2</sub>	1.035	0.005	24.95	0.35	25.31	0.08	25.36	0.25
Al <sub>2</sub> O <sub>3</sub>	0.375	0.041	3.85	0.08	3.78	0.03	3.82	0.04
Fe <sub>2</sub> O <sub>3</sub>					19.12	1.24	16.27	1.58
FeO					43.29	1.20	45.97	1.58
FeO <sup>T</sup>	44.114	0.203	60.03	0.30	(60.49)		(60.60)	
MnO	0.185	0.262	0.45	0.07	0.31	0.04	0.35	0.03
MgO	19.285	0.556	7.06	0.20	7.03	0.04	7.18	0.07
CaO	n.a.		n.a.		n.a.		0.08	0.02
P <sub>2</sub> O <sub>5</sub>	3.544	0.018	0.03	0.06	0.01	0.01	0.01	0.01
Tot	98.697	0.681	96.56	0.40	98.98	0.23	99.19	0.31
At. Fract.								
Si	0.1278	0.0003	0.0011	0.0005	0.0007	0.0001	0.0007	0.0001
Ti	0.0033	0.0000	0.0984	0.0010	0.0959	0.0003	0.0960	0.0007
Al	0.0019	0.0002	0.0239	0.0004	0.0224	0.0003	0.0227	0.0003
Fe <sup>T</sup>	0.1563	0.0007	0.2636	0.0022	0.2548	0.0010	0.2553	0.0015
Mn	0.0007	0.0009	0.0020	0.0003	0.0013	0.0002	0.0015	0.0001
Mg	0.1218	0.0024	0.0553	0.0014	0.0528	0.0003	0.0539	0.0005
CaO	n.a.		n.a.		n.a.		0.0004	0.0001
P	0.0127	0.0000	0.0002	0.0003	0.0000	0.0001	0.0000	0.0000
O	<sup>b</sup> 0.5756	0.0002	<sup>b</sup> 0.5560	0.0003	<sup>d</sup> 0.5720	0.0012	<sup>d</sup> 0.5694	0.0140
Tot	1.0000		1.0001		1.0000		0.9999	
			Cats/4 Oxy		Cats/4 Oxy		Cats/4 Oxy	
Si			0.0076	0.0037	0.0051	0.0005	0.0052	0.0006
Ti			0.7083	0.0069	0.6704	0.0024	0.6747	0.0053
Al			0.0239	0.0004	0.1567	0.0024	0.1594	0.0021
Fe <sup>3+</sup>					0.5066	0.0302	0.4317	0.0404
Fe <sup>2+</sup>			b1.8967	0.0162	1.2754	0.0392	1.3615	0.0521
Mn			0.0144	0.0022	0.0092	0.0012	0.0104	0.0007
Mg			0.3976	0.0101	0.3689	0.0028	0.3787	0.0038
Ca			n.a.		n.a.		0.0300	0.0008
P			0.0012	0.0020	0.0003	0.0004	0.0003	0.0003
Tot Cations			3.1975	0.0035	2.9925	0.0138	3.0249	0.0171

Starting material: 92.6 wt % GM123 (an oxide-olivine rock with minor pyroxene and plagioclase from Iron Mountain), 2.1% graphite, 5.3 % Durango apatite. n.a. not analyzed for.

<sup>a</sup>Analyses by Susan Swapp, University of Wyoming electron microprobe

<sup>b</sup>Oxygen by stoichiometry, assuming all Fe<sup>2+</sup>

<sup>c</sup>Analyses by Gregory Symmes, Stony Brook electron microprobe

<sup>d</sup>Oxygen determined directly

<sup>e</sup>Analyses by A. Fiege and D. H. Lindsley, American Museum of Natural History electron microprobe

SB (1992)<sup>c</sup>

**""Low-Ti" Oxides**

Avg of 2	Std Dev
0.80	0.11
3.29	0.08
0.67	0.02
19.34	0.87
74.06	1.48
(91.46)	
0.21	0.03
1.69	0.31
n.a.	
0.08	0.04
100.14	0.44

0.0045	0.0006
0.0139	0.0003
0.0044	0.0001
0.4305	0.0025
0.0010	0.0001
0.0142	0.0026
n.a.	
0.0004	0.0002
<sup>d</sup> 0.5310	0.0006
1.0000	

Cats/1 Oxy

0.0085	0.0011
0.0262	0.0006
0.0083	0.0002
0.1542	0.0071
0.6564	0.0128
0.0019	0.0002
0.0267	0.0049
n.a.	
0.0005	0.0007
0.8827	0.0022

tain, Wyoming) plus

Table 4. Summary of electron microprobe analyses of Fe-Ti oxides, Oct. 2016. Oxygen measured directly

Sample	45T	64T	54T	39T	38T	37TR
Added Comp.	5% "FeP"	7% Ap	4% C	5% "FeP"	7% Ap	7% Ap
P, GPa	0.5	0.5	0.5	0.5	0.5	0.5
Temp °C	1100	1100	1150	1150	1150	1150
Duration (hrs.)	89.7	70.5	72.6	68.3	69.5	70.2
<b>Wt. %</b>	<b>Avg. of 20</b>	<b>Avg. of 18</b>	<b>Avg. of 21</b>	<b>Avg. of 19</b>	<b>Avg. of 20</b>	<b>Avg. of 20</b>
SiO <sub>2</sub>	0.15(5)	0.14(3)	0.09(5)	0.08(2)	0.06(1)	0.07(1)
TiO <sub>2</sub>	22.37(25)	22.22(29)	29.647(33)	26.76(21)	28.25(29)	28.92(22)
Al <sub>2</sub> O <sub>3</sub>	4.95(4)	5.28(4)	5.21(5)	5.11(6)	4.94(5)	5.21(4)
Fe <sub>2</sub> O <sub>3</sub>	19.06(1.20)	23.68(1.77)	5.20(2.20)	14.17(2.09)	10.36(1.90)	5.93(3.00)
FeO	48.36(1.30)	44.10(1.77)	52.95(2.08)	49.34(1.85)	50.99(1.83)	54.41(2.84)
MnO	0.31(2)	0.32(2)	0.37(3)	0.29(2)	0.33(3)	0.34(3)
MgO	3.17(6)	3.16(4)	4.41(5)	3.28(5)	3.63(4)	3.67(5)
CaO	0.07(2)	0.13(4)	0.05(2)	0.04(1)	0.04(2)	0.09(3)
P <sub>2</sub> O <sub>5</sub>	0.04(2)	0.02(1)	0.00(1)	0.02(1)	0.01(1)	0.01(1)
Tot	98.48(29)	99.04(49)	98.63(45)	99.10(35)	98.61(33)	98.64(29)
<b>Atomic Fraction</b>						
Si	0.0007(2)	0.0007(2)	0.0005(2)	0.0005(1)	0.0003(1)	0.0004(1)
Ti	0.0877(8)	0.0861(9)	0.1141(9)	0.1034(8)	0.1095(9)	0.1121(9)
Al	0.0304(3)	0.0320(2)	0.0314(3)	0.0309(4)	0.0300(3)	0.0316(3)
Fe <sup>T</sup>	0.2856(15)	0.2818(12)	0.2494(16)	0.2668(10)	0.2599(15)	0.2575(19)
Mn	0.0014(1)	0.0014(1)	0.0016(1)	0.0013(1)	0.0014(1)	0.0015(1)
Mg	0.0247(5)	0.0243(3)	0.0336(4)	0.0252(4)	0.0279(3)	0.0282(4)
CaO	0.0004(1)	0.0007(2)	0.0002(1)	0.0002(1)	0.0002(1)	0.0005(1)
P	0.0002(1)	0.0001(0)	0.0000(0)	0.0001(0)	0.0000(0)	0.0001(0)
O	0.5720(13)	0.5759(15)	0.5724(20)	0.5749(16)	0.5740(17)	0.5714(26)
<b>Cats/4 Oxygens</b>						
Si	0.005(1)	0.005(1)	0.003(2)	0.003(1)	0.002(0)	0.003(0)
Ti	0.613(5)	0.598(7)	0.797(7)	0.719(7)	0.763(7)	0.785(9)
Al	0.213(2)	0.222(2)	0.220(3)	0.215(3)	0.209(3)	0.221(3)
Fe <sup>T</sup>	1.997(15)	1.958(13)	1.743(17)	1.856(11)	1.811(15)	1.803(22)
Mn	0.010(1)	0.010(1)	0.011(1)	0.009(1)	0.010(1)	0.010(1)
Mg	0.172(4)	0.169(2)	0.235(3)	0.175(3)	0.195(3)	0.197(3)
Ca	0.003(1)	0.005(2)	0.002(1)	0.001(1)	0.002(0)	0.003(1)
P	0.001(0)	0.001(0)	0.000(0)	0.000(0)	0.000(0)	0.000(0)
Tot Cations	3.014(16)	2.967(18)	3.012(24)	2.980(19)	2.992(20)	3.023(32)

Analyses by A. Fiege and D. H. Lindsley, American Museum of Natural History. Oxygen determined directly. Standards: Fe, Ti, O: Synthetic Usp<sub>50</sub>Mt<sub>50</sub>; Mg, Si, Ca: diopside; Al: orthoclase; P: berlinite. Numbers in ( ) show detection limits (ppm): O, 2700; Mg, 260; Al, 290; Si, 220; P, 170; Ca, 160; Ti, 800; Mn, 530; Fe, 770. ORT, Bolsover's oxide-rich troctolite SCP-113. xxT indicates experiments on unreduced ORT starting material reduced at 1040°C and at fO<sub>2</sub> "within the fayalite stability field". ORE, see text. Fe<sup>T</sup>, total iron. Added components are: C, synthetic graphite. "FeP", synthetic Fe<sub>4</sub>(P<sub>2</sub>O<sub>7</sub>)<sub>3</sub>. Ap, fluorapatite.

61 ORE	Usp <sub>70</sub> GrAp(4)	GM123-14	Usp <sub>50</sub> Mt <sub>50</sub>
oxalic acid	4% C 16% Ap	2.1% C 5.3% Ap	(Synthetic) working standard)
0.5	0.5	0.5	
1200	1250	1308	
unk	15	24	
<b>Avg. of 20</b>	<b>Avg. of 20</b>	<b>Avg. of 20</b>	<b>Avg. of 10</b>
0.09(2)	0.07(2)	0.15(2)	0.29(1)
27.54(28)	25.30(28)	25.36(25)	17.39(32)
5.13(7)	0.00(0)	3.82(4)	0.00(0)
15.74(2.63)	24.24(1.56)	16.27(1.58)	32.41(2.16)
4.96(2.45)	49.57(1.64)	45.97(1.58)	49.37(2.19)
0.39(3)	0.02(2)	0.35(3)	0.01(2)
3.07(5)	0.04(1)	7.18(7)	0.02(2)
0.03(1)	0.40(11)	0.08(2)	0.02(1)
0.03(1)	0.05(6)	0.01(1)	0.03(1)
98.98(49)	99.68(50)	99.32(36)	99.53(31)
0.0005(1)	0.0004(1)	0.0007(1)	0.0016(1)
0.1062(9)	0.1020(17)	0.0877(8)	0.0877(8)
0.0310(5)	0.0000(0)	0.0229(3)	0.0000(0)
0.2622(15)	0.3202(21)	0.2553(15)	0.3541(71)
0.0017(1)	0.0001(1)	0.0015(1)	0.0001(1)
0.0235(4)	0.0003(1)	0.0539(1)	0.0001(1)
0.0002(1)	0.0023(6)	0.0004(1)	0.0001(1)
0.0001(1)	0.0002(3)	0.0000(0)	0.0001(0)
0.5779(22)	0.5769(16)	0.5695(14)	0.5714(34)
0.003(1)	0.003(1)	0.005(1)	0.011(1)
0.736(8)	0.708(4)	0.675(5)	0.500(6)
0.215(4)	0.000(0)	0.159(21)	0.000(0)
1.815(17)	2.220(21)	1.793(14)	2.507(31)
0.012(1)	0.000(0)	0.010(1)	0.000(1)
0.163(3)	0.002(1)	0.379(4)	0.001(1)
0.001(0)	0.016(4)	0.003(1)	0.001(1)
0.000(0)	0.001(2)	0.000(0)	0.001(0)
2.944(27)	2.950(19)	3.025(17)	3.021(28)

Conditions, 15 kV, 20 nA. Beam 5 microns.  
 low standard deviation in the last decimal place(s).

ial. xxTR indicates experiments on ORT that had been  
 iron.

e from Durango, Mexico.



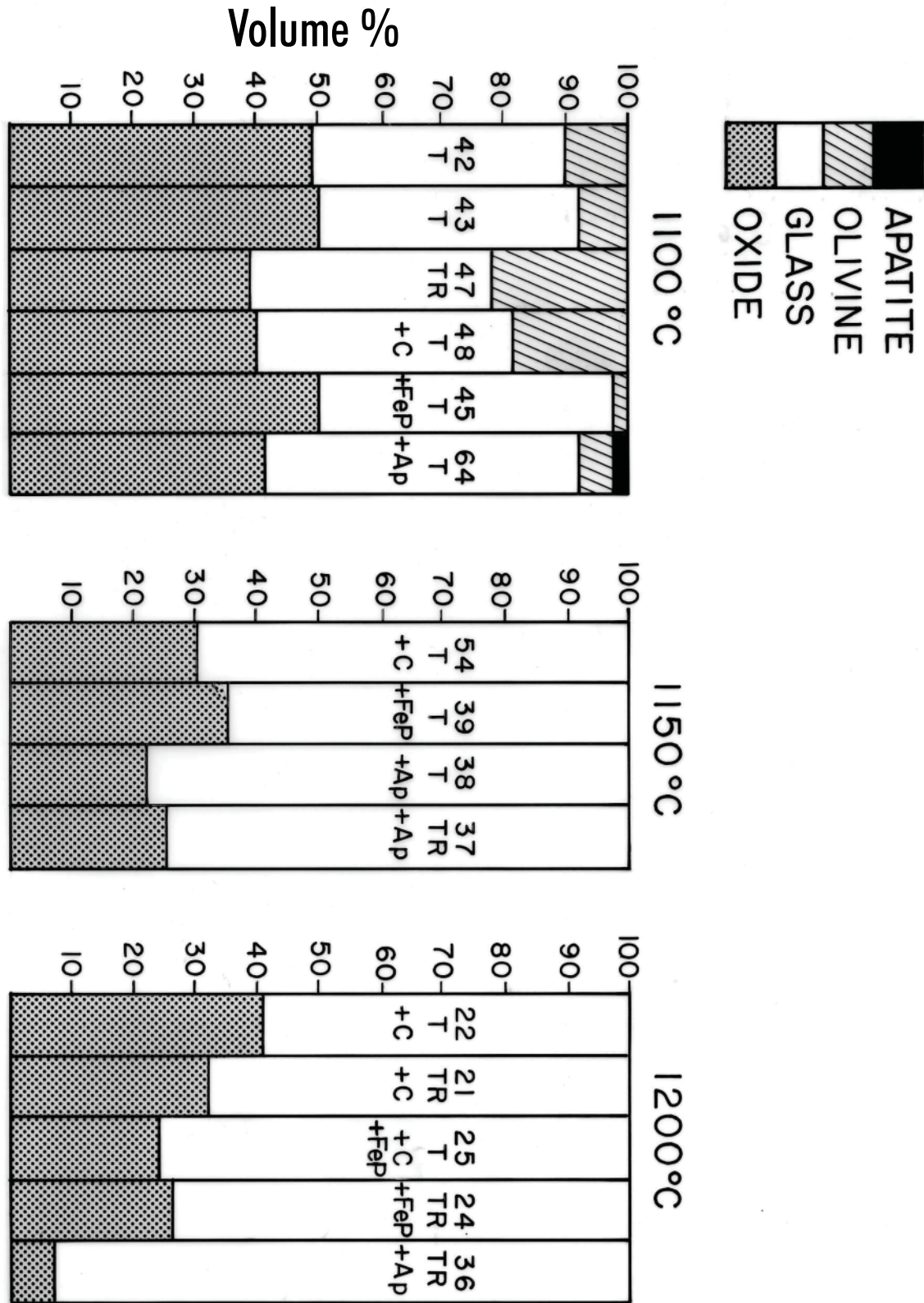
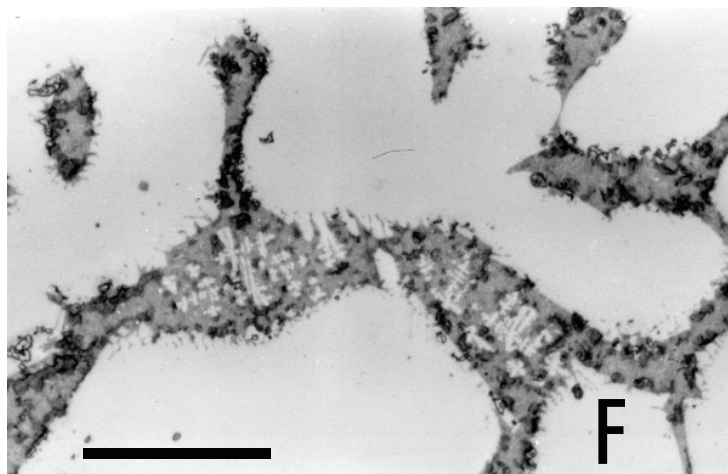
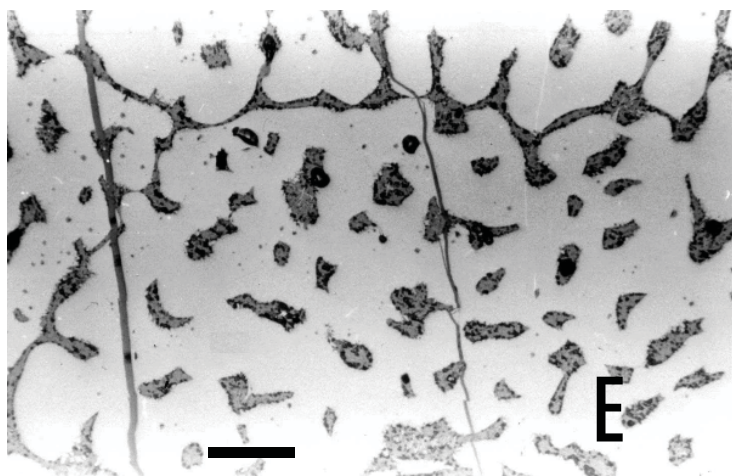
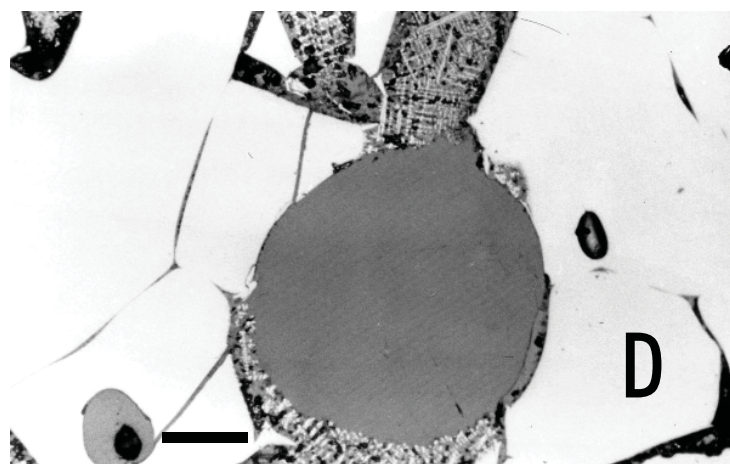
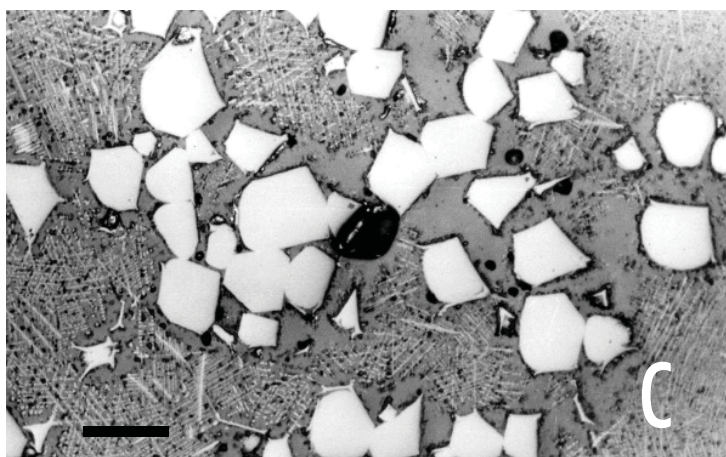
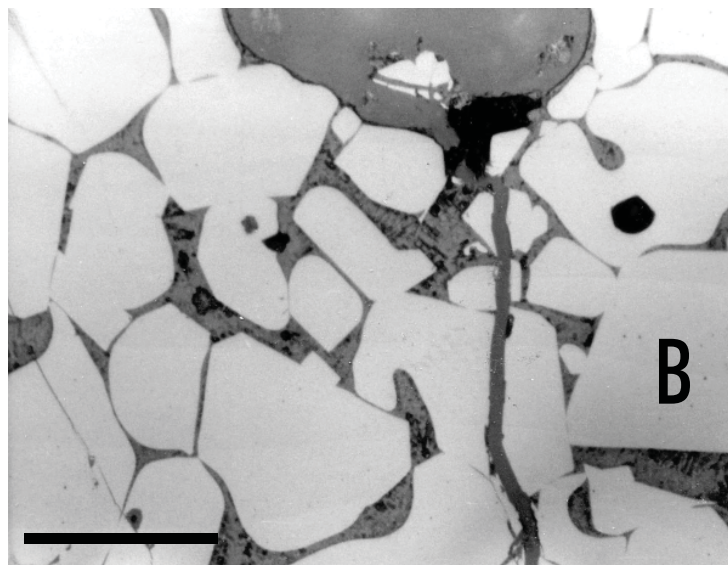
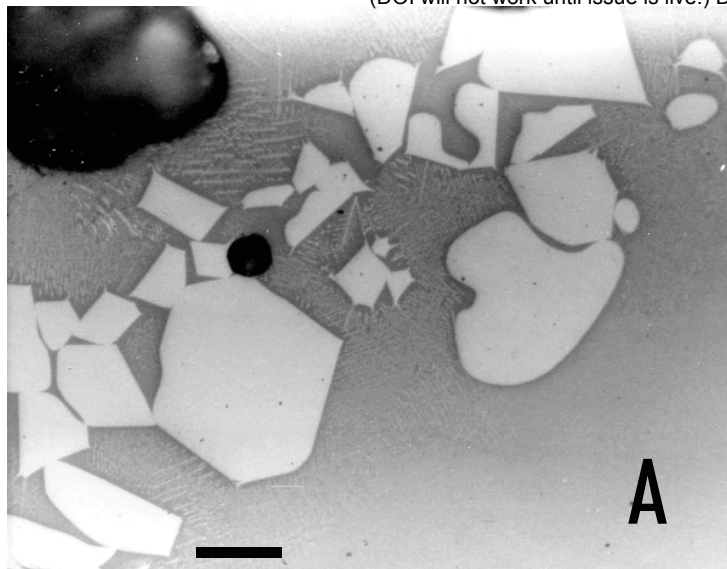
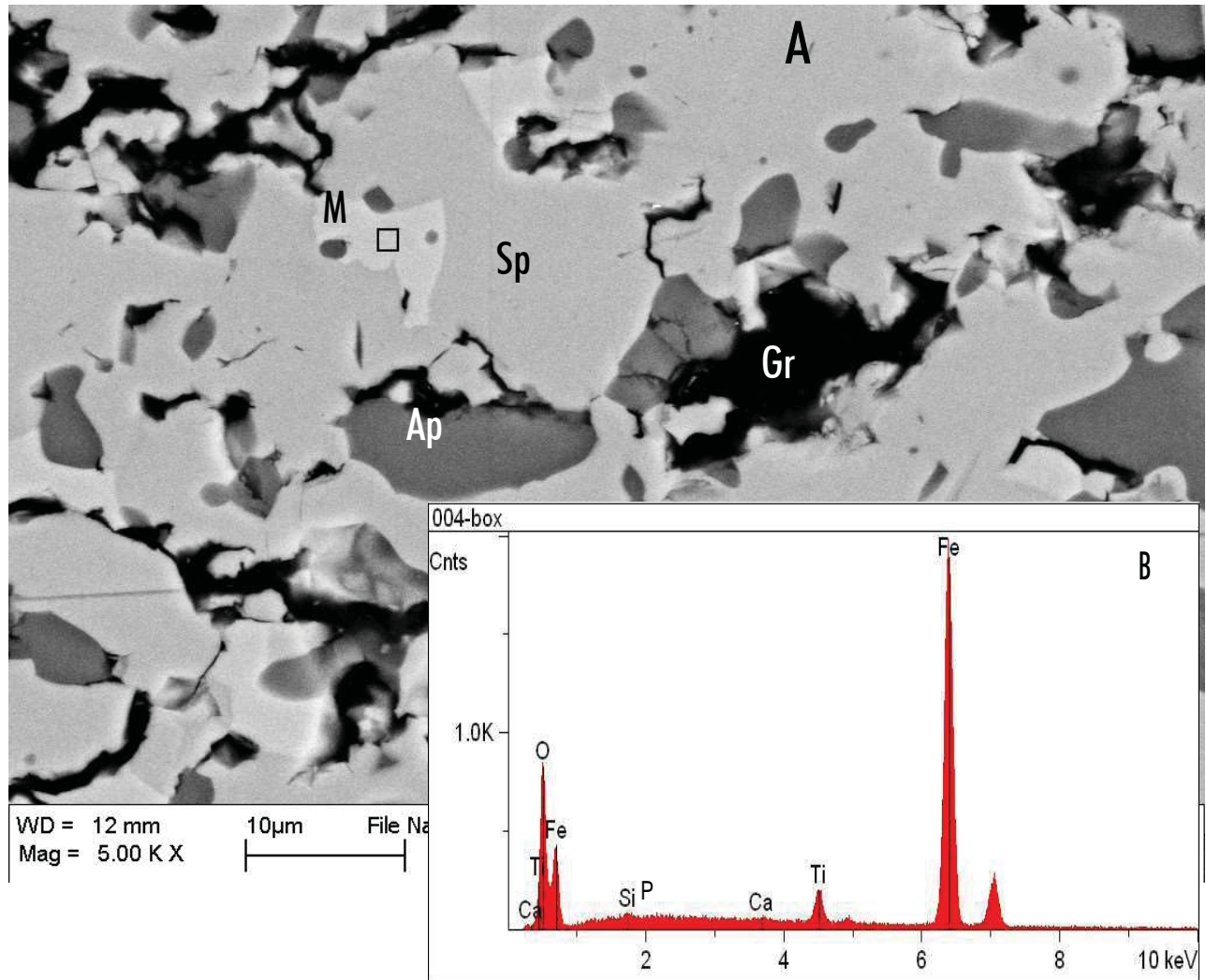


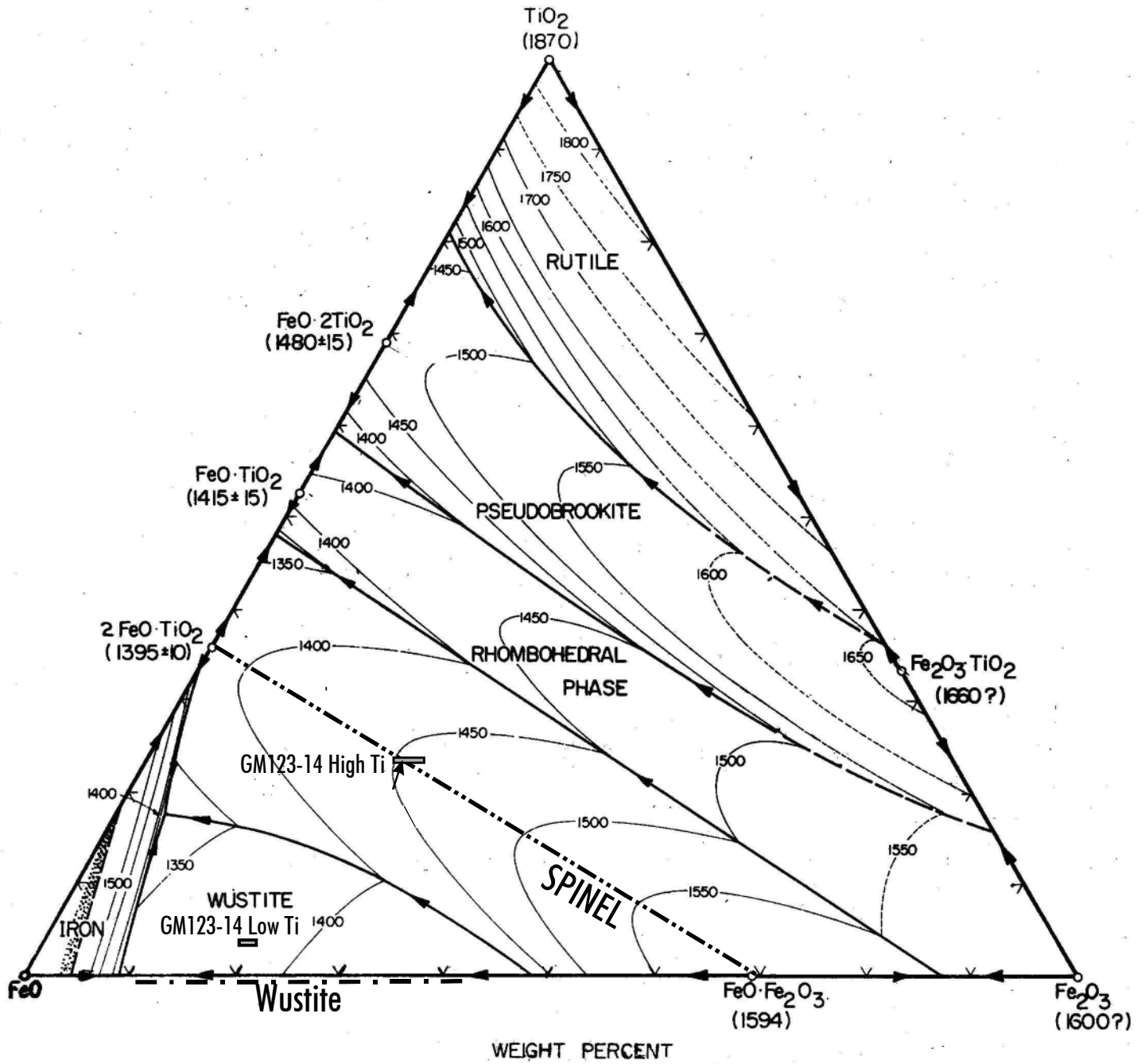
**Fig. 1**



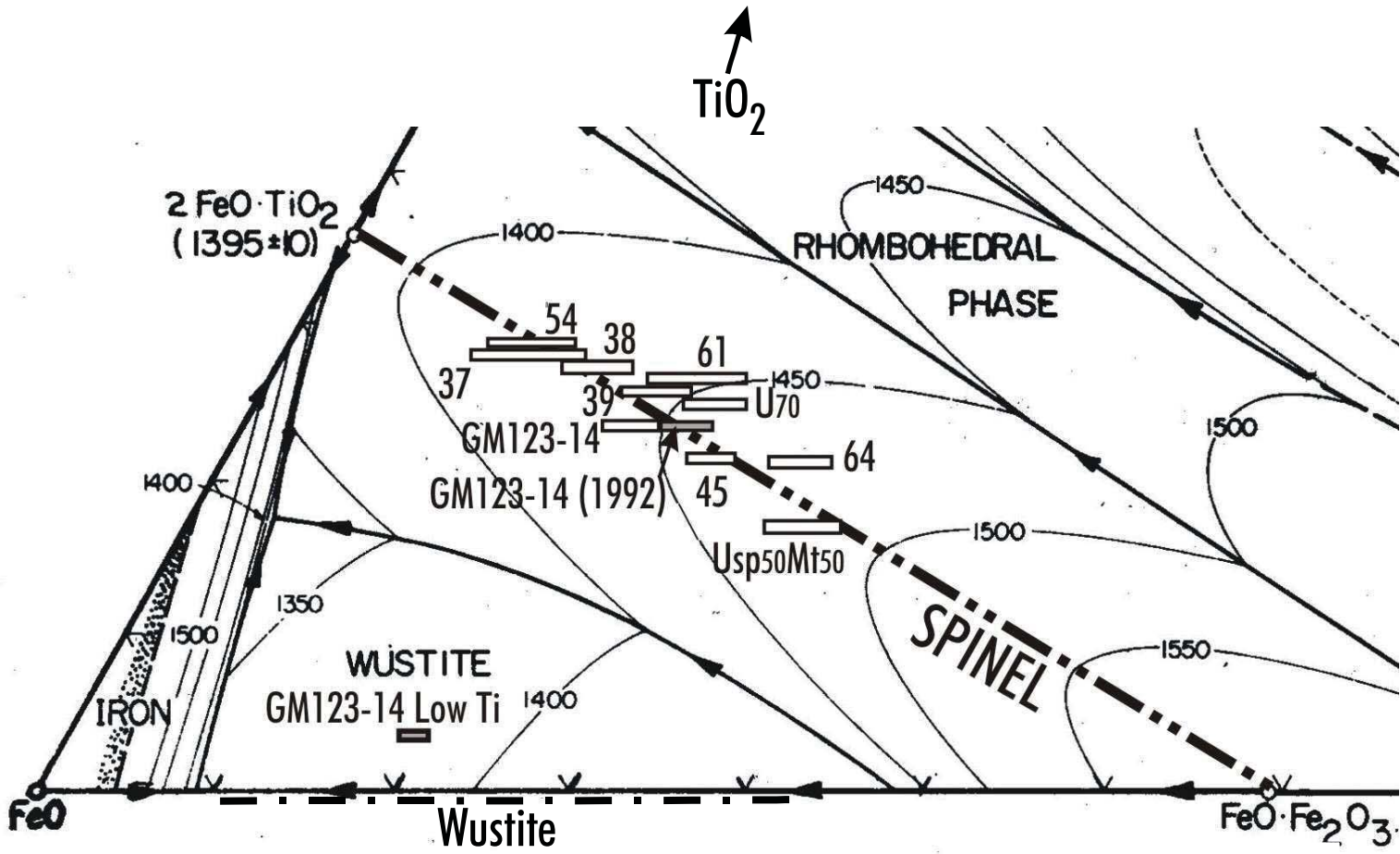
Lindsley-Epler Fig. 2



Lindsley-Epler Fig. 3



Lindsley-Epler Fig. 4



Lindsley-Epler Fig. 5

